SEISMIC RISK ASSESSMENT OF HIGH-VOLTAGE TRANSFORMERS USING BAYESIAN BELIEF NETWORKS

by

Tammeen Siraj

B.Sc., Bangladesh University of Engineering & Technology, Bangladesh, 2009

A THESIS SUBMITTED IN PARTIAL FULFILLMENT OF

THE REQUIREMENTS FOR THE DEGREE OF

MASTER OF APPLIED SCIENCE

in

THE COLLEGE OF GRADUATE STUDIES

(Civil Engineering)

THE UNIVERSITY OF BRITISH COLUMBIA

(Okanagan)

April 2013

Abstract

Past earthquake records showed that a large magnitude earthquake can cause severe damage to high-voltage substations, which may lead to power disruption for a significant amount of time. A high-voltage transformer is one of the key components of a substation. This thesis proposes a probabilistic framework using Bayesian belief network (BBN) model to predict the vulnerability of a high-voltage transformer for a seismic event. BBN has many capabilities that make it well suited for the proposed risk assessment method. This thesis considers past studies, expert knowledge and reported causes of failures to develop an initial integrated risk assessment framework that acknowledges multiple failure modes. Therefore, the framework incorporates major causes of transformer vulnerability due to seismicity, such as liquefaction, rocking response of transformer, or interaction between interconnected equipment. To demonstrate the application of this framework, this thesis elaborates each step of the framework. Finally, the sensitivity analysis was carried out to evaluate the effects of input variables on transformer damage. The paper also illustrates two predictive models using response surface method (RSM) and Markov chain. The proposed framework is particularly handy to perform, and the results can be useful to support decisions on mitigation measures and seismic risk prediction.

Table of Contents

List of Tables

List of Figures

List of Notations

BBN	Bayesian belief network
PGA	Peak ground acceleration
IC	Interaction coming from the conductors
RT	Rocking response of transformer
M_w	Earthquake magnitude
d	Site to fault distance
S_T	Soil type
F_M	Fault mechanism
EL	Extremely low
VL	Very low
L	Low
M	Medium
H	High
VH	Very high
EH	Extremely high
EEH	Extremely extremely high
D_{50}	Average grain size
q_c	CPT tip resistance
σ_{vo}	Effective vertical overburden pressure
σ'_{vo}	Effective vertical overburden pressure
D_{rel}	Maximum horizontal relative displacement between adjacent equipment
μ_s	Static coefficients of friction
B/H	Width to height ratio of transformer
RSM	Response surface method

Acknowledgements

In the name of Allah, the Most Gracious and the Most Merciful

All praises go to the almighty Allah to give me the strength and his blessing in completing this thesis. I express my sincere gratitude to my supervisor, Dr. Solomon Tesfamariam, who has inspired and guided me all through my MASc program. I would like to thank him for his believe in my potential. His constructive comments and suggestions throughout the thesis works have made a significant contribution to the success of this research.

I offer my enduring gratitude to the faculty, and staff at the UBCO. I would also like to acknowledge Natural Sciences and Engineering Research Council of Canada (NSERC)'s support in this research work. I owe particular thanks to Dr. Leonardo Dueñas-Osorio and Dr. Goutam Mondal, whose invaluable suggestions taught me to question more deeply.

Special thanks are owed to my parents for all their love, patience, and encouragement. They are the key source of inspiration for all my achievements. I am also thankful to those who indirectly contributed in this research, your kindness means a lot to me.

DEDICATED TO MY PARENTS

উৎসর্গ করলাম আমার আব্বু ও আম্মুকে।

Chapter 1: Introduction

An electrical power transmission system is comprised of power generating stations, substations, transmission lines, and supervisory control and data acquisition (SCADA) facilities. Substations connect all other components (Figure 1.1) and transfer powers in different voltage levels. They perform many functions such as: change AC voltages from one level to another; switch generators, equipment, and circuits or lines in and out of a system, etc. Substations are comprised of different components, e.g., disconnect switch, circuit breaker, transformer, lightning arrester, control house, protection and control equipment (Blume 2007).

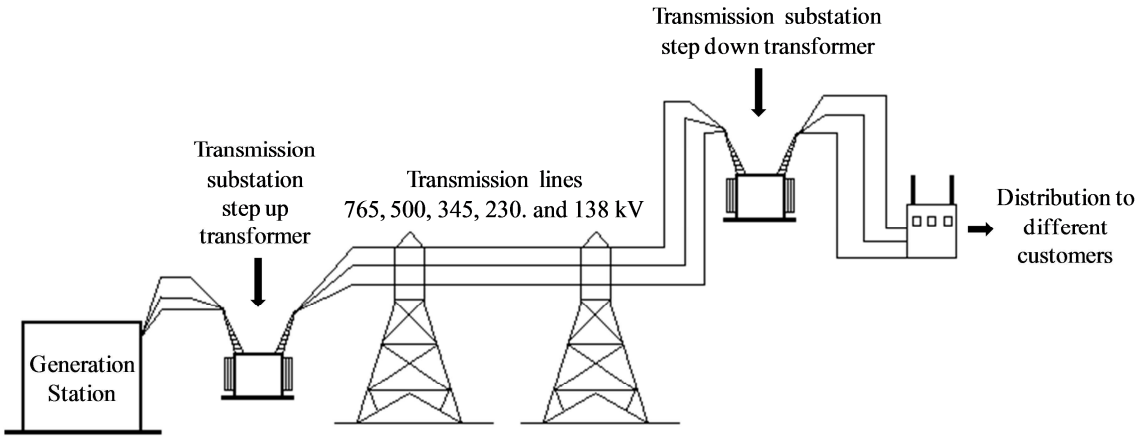

Figure 1.1 Basic structure of power system (Adapted from United States Department of Energy (2004))

Seismic shaking may cause damage to the substations in a power system. Failure of an electrical substation can cause power outages of varied amounts of time (Table 1.1). The consequence of those substation damages can lead to several hours of power outage and monetary loss. Table 1.1 presents a summary of power disruption and monetary loss during major earthquakes.

Table 1.1 Summary of power disruption and monetary loss due to substation damage during major earthquakes

Earthquakes	Magnitude	Power Disruption and Monetary Loss
1988, Saguenay earthquake	5.9	Power outages in Quebec City; complete power restoration occurred 9 hours after the earthquake (Mitchell et al. 1990).
1989, Loma Prieta earthquake	6.9	Electricity was lost to about 1,400,000 customers due that earthquake (Schiff 1998).
1994, Northridge earthquake	6.7	Power outages in Los Angeles area lasted from a few seconds to several days; power restoration was done to all major substations and to about 95% of the customers within 24 hours (Schiff 1997).
2010, Christchurch earthquake	7.1	It took a day to achieve 90% restoration during that earthquake (Eidinger and Tang forthcoming).
1971, San Fernando Earthquake	6.6	Estimated loss $22,000,000 due to component damage of Sylmar Converter station (500 kV DC), or 40 percent of the total value of loss (Eidinger and Ostrom 1994).

1.1 Motivation

Experiences from past earthquake records showed that large magnitude earthquakes could cause severe damage to substations and result in major service disruption of a power system. High-voltage substation components that have been designed without full consideration of the site seismicity and/or designed before the introduction of modern seismic design codes are the most vulnerable (Anagnos 1999). The commonly observed failure modes could be listed as failures in transformer anchorage, oil leakage from bushings and different parts of the transformers, shattering of porcelain columns, etc. Given diverse classes of assets exposed to seismic hazard, consistency in the process of risk assessment and management becomes a challenging task (Nuti et al. 2007). A key component of a substation is the transformer which is one of the single largest capital investments (60% of the total investment). Hence, replacing a damaged transformer with a new one or keeping a spare transformer in a substation is expensive. Also, according to the past earthquake observation,

the damage rate of high-voltage transformer is low, but their failure has high consequences (Abdelmoumene and Bentarzi 2012; Gaunt and Coetzee 2007); therefore seismic risk assessment of a transformer is of vital importance. Since, Bayesian belief network (BBN) takes into account the uncertainty in the modeling and aggregation of the different knowledge base, this thesis demonstrates a risk assessment framework using Bayesian belief network for high-voltage transformers in a substation.

This thesis uses seismic vulnerability and risk in an alternative way as the definition of the vulnerability follows the same logic as that of risk (Aven 2008). Risk is related to future events (i.e., a seismic event) and their consequences (i.e., failure of substation components), and vulnerability is related to the combination of consequences (i.e., failure of substation components) and associated uncertainty (i.e., uncertainty of the consequences). Therefore, vulnerability is a feature of risk (Aven 2008).

Risk assessments are crucial as they reduce the risks of unwanted events, which could be very costly both physically and financially. It is essential for Governments and decision makers to evaluate the seismic risk of substations. It directly contributes to the improvement of safety and security in a power system against seismic hazard of varying magnitudes.

1.2 Objective and Organization of the Thesis

The objective of this research is to develop a risk assessment framework for high-voltage transformers by combining current knowledge in the areas of seismic hazard. This thesis includes the use of conventional methodology to quantify site seismicity and the other effects that may induce from site seismicity (i.e., liquefaction, rocking response, conductor interaction of the interconnected equipment). Finally, a risk assessment framework is

developed to quantify the probability of failure of a high-voltage transformer using Bayesian belief network in the event of an earthquake.

The thesis is divided into five chapters. **Chapter 1** introduced the study by describing the objectives and motivation. **Chapter 2** presents a state of the art review, explaining the past earthquake performances of substations. The chapter also discusses previous vulnerability studies on substations and its components. Later in this chapter, basics of risk assessment and a brief idea of Bayesian belief network are discussed.

Chapter 3 elaborates on the proposed framework using Bayesian belief network and the sensitivity analysis using the proposed framework. **Chapter 4** presents the predictive model development using response surface method and Markov chain separately. Finally, **Chapter 5** presents a summary of the research and the conclusions. In addition, limitations of the current study and suggestions for future improvement are also presented in this chapter.

Chapter 2: Literature Review

High-voltage equipment (e.g., porcelain members, transformers, bushing) are the most vulnerable parts of the substation during an earthquake (Anagnos 1999). Performance evaluation of high-voltage substation equipment during a seismic event has become a crucial issue. For substations and its components, this chapter reviews past earthquake induced damage and current state of practice on vulnerability assessment. Finally, a brief review of risk assessment, with more emphasis on Bayesian belief network, is provided.

2.1 Past earthquake performance of high-voltage substation components

Typically, voltage rating of components of a substation is one of the factors that are related to its seismic vulnerability (Stewart et al. 2003). Equipment with 115kV or below showed satisfactory performance during past earthquakes, if seismic installation practices of anchorage and conductor interconnection flexibility were present (Anagnos 1999). Different types of damages in substations observed from the past earthquake records are (ASCE 1999; Schiff 2003):

- Leaking or breaking of bushing,
- Falling of inadequately anchored rail-supported transformers from the elevated platforms,
- Damage of bushings and post insulators,
- Failure of cast-aluminum hardware,
- Failure of porcelain insulator,
- Tilting of lighting arresters, and
- Tilting of dead end transmission tower.

Past earthquake records showed that damage to substation components may lead to severe consequences. For example, the 1994 Northridge earthquake caused severe damage to the electric power facilities of Los Angeles. The damage to electric power could have far

reaching consequences, as well. British Columbia, Montana, Wyoming, Idaho, Oregon and Washington experienced power outages due to the damage to substations in the Los Angeles area (Anagnos 1999; Schiff 1997). The Los Angeles Department of Water and Power's (LADWP) Sylmer Converter Station suffered severe damage (Figure 2.1) that included transformer bushings, lightning arresters, disconnect switches, circuit switchers, bus supports, and potential measuring devices (Eidinger and Ostrom 1994). Similar damages were found in the 1988 Saguenay earthquake, the 1989 Loma Prieta earthquake, the 1995 Kobe earthquake, the 2010 Christchurch earthquake, etc.

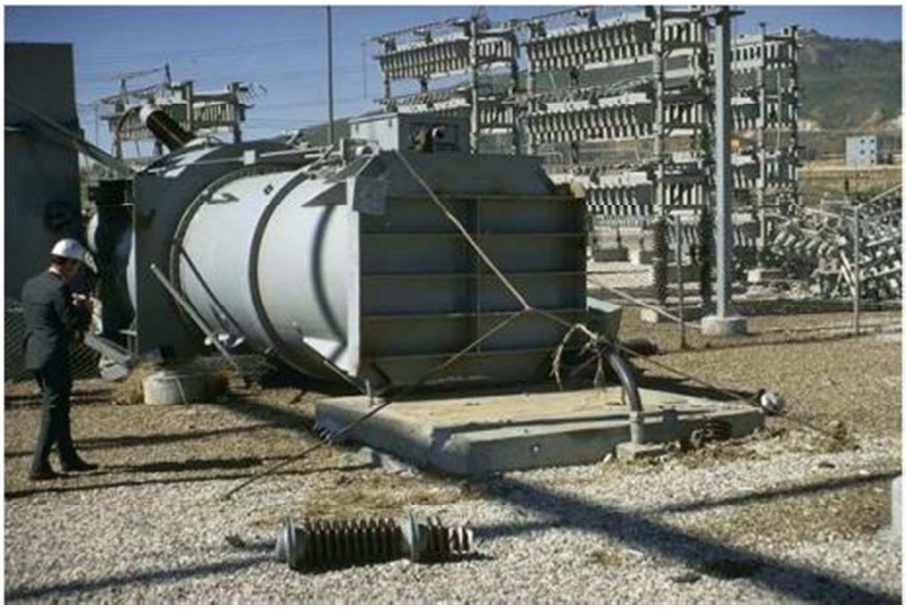

Figure 2.1 Overturned electrical equipment at Sylmar Converter Station during 1971 San Fernando earthquake (Magnitude 6.6) (Makris and Zhang 1999)

Several components of transformers were also found damaged from different earthquakes (ASCE 1999). These include damage to anchorage, radiators, bushings, conservators, lightning arresters, sudden pressure and protective relays, tertiary bushings, etc. Figure 2.2 shows a photograph of a broken transformer bushing during the 2010 Christchurch earthquake. Also damages due to liquefaction were reported (Eidinger and Tang

forthcoming). Among 300 substations in Christchurch, two of the substations failed to operate due to liquefaction.

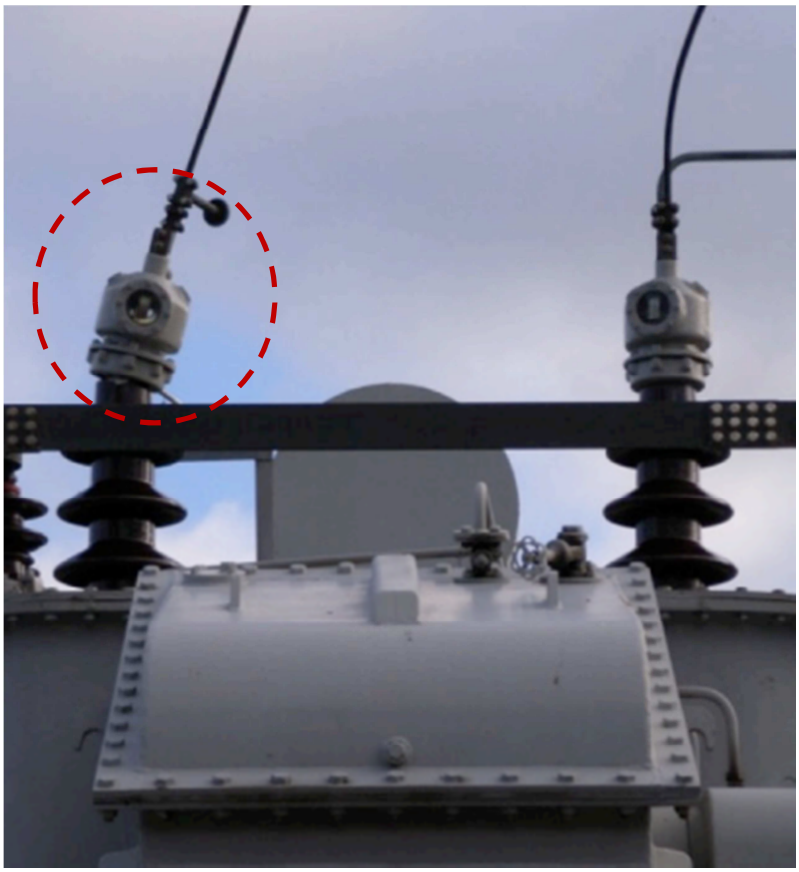

Figure 2.2 66 kV broken transformer bushing at Bromley substation during 2011 Christchurch earthquake (Magnitude 6.3), (Eidinger and Tang forthcoming)[1]

Based on the past performance of electrical substation components, it is evident that, mitigation measure has to be performed to improve performance during an earthquake. Recently, many substations are in the process of implementing mitigation measures which have performed relatively well during an earthquake event. For example, the electrical power companies in New Zealand implemented mitigation measures to some of the substations and

[1] With permission from American Society of Civil Engineers (ASCE)

as a result, the substations performed relatively well during the Christchurch earthquake (2010) (Eidinger and Tang forthcoming). During the 1994 Northridge earthquake, it was also observed that equipment designed after the 1971 San Fernando earthquake suffered less damage comparing to older equipment (Jaigirdar 2005).

2.2 Previous vulnerability studies on substation

Several experimental and analytical studies have been conducted for evaluating the seismic performance of different substation components. A list of different substation vulnerable studies is shown in Table 2.1.

Table 2.1 Studies on vulnerability assessment of substation components

Substation components	Reference
Transformer and bushing system	Ersoy (2002); Ashrafi (2003);Ersoy and Saadeghvaziri (2004); Saadeghvaziri et al. (2010); Ersoy (2001); Filiatrault and Matt (2006)
Rocking response and overturning of equipment	Makris and Roussos (1998); Makris and Zhang (1999)
Rigid electrical equipment anchored to a base foundation (e.g., transformer)	Makris and Black (2001, 2002)
Electrical substation equipment connected by non-linear rigid bus conductors	Song et al. (2007)
Cable-connected equipment items	Hong et al. (2001)
High-voltage disconnect switch	Paolacci and Giannini (2009)
550 kV porcelain transformer bearings	Gilani et al. (1999a)
230-kV porcelain transformer bushings	Gilani et al. (1999b)
High-voltage substation disconnect switches	Whittaker et al. (2007)
High-voltage transformer-bushing systems	Whittaker et al. (2004)

The previous vulnerability studies showed that the analytical and experimental works are undertaken for a particular failure mode. Song et al. (2007) and Hong et al. (2001) worked on the response of cable connected equipment; Ersoy and Saadeghvaziri (2004)

worked on seismic interaction of transformer and bushing system; Makris and Roussos (1998) worked on rocking response and uplifting of equipment, etc. Combining all the failure modes together will be a challenging task, but it will help to start integrating such diversity of failure modes to give a better understanding on component vulnerability. Other studies that have been performed related to substation and its components vulnerability are discussed in the following paragraphs.

Anagnos (1999) developed fragility curves for different equipment of a substation for specific types of failure modes. Data from twelve earthquakes which occurred between 1971 and 1994 was used to develop these fragility curves. Anagnos (1999) did not consider the statistical dependence among the observations while estimating the equipment fragilities. The dependency mainly comes when any equipment experiences multiple earthquakes. Straub and Der Kiureghian (2008) showed that the conventional approach of fragility estimation using the past earthquake damage data differs significantly if they introduce effects of statistical uncertainty and component statistical dependence on the system fragility. Developing fragility curves based entirely on the available damage data is not always sufficient as damage data is not enough to adequately define a fragility curve (e.g., there could be lack of data or incomplete data or missing failure modes) (Anagnos 1999).

On the other hand, Hwang and Chou (1998) used risk assessment tools (i.e., fault tree and event tree) to evaluate the performance of an electrical substation for a seismic event. In their study, fault tree and event tree demonstrate the interrelationship between the substation components. Fragility of a substation was determined by using the fragility of individual components in event tree and fault tree. The fragilities of individual components were determined by analytical or experimental analysis by Huo and Hwang (1995).

Matsuda et al. (1991) developed a method to assess substation damage and system impacts during an earthquake event. The method includes, 1) identifying scenario earthquake (high probability, large magnitude earthquake), 2) selecting and ranking the substations based on their exposure to scenario earthquakes and their importance to the system, 3) performing additional assessment on highest ranked substations, 4) assessing damage on the system due to scenario earthquakes, and 5) finally, developing seismic hazard mitigations. Their methodology was tested and verified for the Loma Prieta earthquake. Their assumptions were that 1) soil condition has a significant effect on substation components, 2) dead tank and bulk oil circuit breakers would not be damaged during the earthquake, 3) most of the damage would occur to the 500kV substation equipment, and 4) substation equipment below 115kV voltage level was unlikely to be damaged. Those assumptions matched with the actual scenario during the Loma Prieta earthquake.

The previous studies reflected that work has been done to assess vulnerability of substation as a whole and its individual components. To evaluate the whole substation vulnerability, it is essential to get an idea of the vulnerability of its components. Vulnerability assessment of substation components could also be achieved by using risk assessment tools, other than developing analytical model or experimental analysis. When it comes to measuring the seismic risk of substations on a vast scale, analytical and experimental work may not be suitable. As analytical model is time consuming and computationally intensive, on the other hand, experimental work is expensive. The following section discusses the basics of risk assessment.

2.3 Methods for risk assessment

In a very broader sense, risk can be defined as the combination of the probability, or frequency, of occurrence and the consequence of a specific hazardous event (Sušnik et al. 2010). While doing risk assessment, it is necessary to integrate knowledge with diverse nature (i.e., qualitative and quantitative). Risk assessment can be done by specially focusing on qualitative knowledge. For example, organization and human analyses are more naturally modeled with qualitative knowledge and some of the qualitative techniques of risk assessment are Hazard and Operability Analysis (HAZOP), *what-if* analysis, preliminary risk analysis, Hazard Assessment Critical Control Points (HACCP), etc (Aven 2008). On the other hand, technical level risk assessment is usually modeled with quantitative information. There are several quantitative risk assessment techniques such as, Fault Tree Analysis (FTA), Event Tree Analysis (ETA), Failure Mode and Effects Analysis (FMEA), barriers and bow-tie diagrams, etc. (Aven 2008).

For seismic risk assessment of critical substation component (i.e., transformer in this thesis), the main characteristics to be modeled are stochastic behavior of earthquake ground motion (Song et al. 2004), induced effects from ground motion (i.e., liquefaction, rocking response) (ASCE 1999), behavior and performance of interconnected equipment (Der Kiureghian et al. 1999a), the complexity of the equipment itself, the integration of qualitative information with quantitative knowledge, the multi-state nature of equipment, the dependencies between events such as failures, and uncertainties on the parameter estimation (Weber et al. 2010), etc. Thus, classical dependability (i.e., availability, safety, reliability, maintainability, integrity) analysis methods, such as failure mode and effect analysis (Abdelgawad and Fayek 2012), fault trees (Bobbio 1999; Porter et al. 2006), Markov chains

(Yi et al. 2011), Petri nets (Wakefield and Sears 1997), and Bayesian belief networks (BBN) (Bensi et al. 2011; Liu et al. 2011), can be used.

The BBN provides a robust probabilistic method of reasoning under uncertainty (Bobbio et al. 2001). Recent literature shows a growing interest on BBN, because of its usefulness in risk assessment of complex systems (Boudali and Dugan 2005; Langseth and Portinale 2007; Mahadevan et al. 2001). A brief discussion of each method with relation to BBN is provided in the following paragraphs. The discussions highlights that BBN has many capabilities that make them well suited for the risk assessment of substation components. This thesis uses the BBN as a risk assessment tool to perform vulnerability assessment of high-voltage transformers. It has been successfully applied in a variety of real-world tasks, and their suitability for risk assessment is considered by several researchers (e.g., Bensi et al. 2011; Liu et al. 2011; Tesfamariam and Liu 2013; Tesfamariam et al. 2011).

Failure mode and effect analysis (FMEA) techniques are widely used to identify potential failure modes, to assess the risk associated with those failure modes, to rank the issues in terms of importance and to identify and carry out corrective actions to address the most serious concerns (Lee 2001). FMEA is an effective fault analysis technique but the ability of inference is not very enough and FMEA method is not suitable to use the fault related symptoms to do some posterior inference (Yang et al. 2009). In addition to that, this method is difficult to use in decision making and reuse, on contrary BBN is excellent at them (Chen et al. 2010). BBN can be constructed from FMEA and the events that cannot be done in FMEA, BBN takes care of them (Shi and Wang 2004; Yang et al. 2009).

Fault tree (FT) analysis is one of the most popular techniques for dependability analysis. The FT is a graphical model of various combinations of faults that may present as parallel and sequential way, which will result in the occurrence of the predefined undesired event. FT can easily be mapped into a BBN. By using BBN in comparison with FT, it is possible to obtain some additional power both at modeling and at the analytical level. Bobbio (1999) explained the different issues of FT and BBN. FT analysis could give exactly the probability of failure of a system or equipment. The problem arises when it deals with multiple failure of components that lead to several different consequences on the system (Weber et al. 2010). That is a common case in risk and dependability analysis, and those models need to be represented by multiple state variables. In that context, FT is not a preferable option. Another problem with FT analysis is that, it is limited to one top event. On the other hand, BBN has the similar capabilities as FT; in addition, BBN allows us to do multistate variable modeling and enables us to assess several output variables in the same model. Therefore, it is possible to represent FT as BBN, but the reciprocity is not always true.

Markov chain (MC) is another suitable method for reliability (i.e., continuity of correct service of the system), and availability (i.e., readiness for correct service of the system) studies of systems. The analysis evaluates exact failure probability, even if there is presence of dependencies among components. It is possible to integrate diverse knowledge and to represent multistate variables with the help of MC. One of the main disadvantages of MC is the analysis becomes complex when a large number of variables are considered (De Souza and Ochoa 1992). On the other hand, BBN takes care of that issue since the parameters in conditional probability table becomes considerably low as compared to MC

(Weber et al. 2010). Later in this thesis, MC has been used to develop the simplified predictive model.

Stochastic Petri Networks (SPNs) are considered as a traditional method to model reliability, availability etc.(Balakrishnan and Trivedi 1996).This is a powerful modeling process except that the reliability analysis method includes a rigorous simulation procedure. Therefore, SPN using simulation methods has two disadvantages: inefficient consideration of low frequency events and the simulation time (Weber et al. 2010). It is essential to consider low frequency events in risk analysis process as accidents are rare events with high consequences. In addition, SPNs do not allow integrating evidence easily, whereas BBN takes into account these events.

As in the case with most computational methods, the limitation with BBN is that the calculations can be highly demanding when the BBN is densely connected (Bensi et al. 2011). A basic idea of BBN is given in the following section.

2.4 Bayesian belief network

Bayesian belief network (BBN) is a graphical model that allows a probabilistic relationship within a set of variables (Pearl 1988). A BBN consists of a directed acyclic graph (DAG). Here, the nodes represent variables of interest with several possible states, and the links between them indicate probabilistic cause-effect relationship among the variables. The uncertainties in a BBN model are reflected through subjective probability (Pearl 1988; Liu et al. 2011; Tesfamariam et al. 2011). The relations between the variables in a BBN are expressed in terms of family relationships, wherein a variable A and B is said to be

the parent of C, and C the child of A and B if the link goes from A to C and B to C (as shown in Figure 2.3). Based on Figure 2.3, a BBN may be formulated by the following steps;

1. Variables necessary and sufficient to model the problem framework of interest are identified (e.g., variable A, B, and C).
2. Causal interrelations existing between the nodes A, B, and C are formulated, graphically shown by arrows.
3. A number of discrete mutually exclusive states are assigned to each variable (e.g., A and B has two states, state I and state II, and C has three states state I, state II and state III).
4. The network supports the computation of the probabilities of any subset of variables (e.g., variable C) given evidence about any other subset (e.g., variable A and variable B). These dependencies are quantified through a set of conditional probability tables (CPTs); each variable is assigned a CPT of the variable given its parents.

Variable A	**Probability**
State I	P_1
State II	P_2

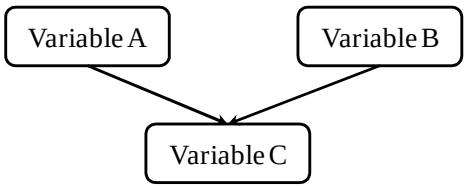

Variable B	**Probability**
State I	P_3
State II	P_4

Variable A	**Probability**	**Conditional probability of variable C**		
		State I	State II	State III
State I	State I	P_5	P_9	P_{13}
State I	State II	P_6	P_{10}	P_{14}
State II	State I	P_7	P_{11}	P_{15}
State II	State II	P_8	P_{12}	P_{16}

Figure 2.3 A sample Bayesian probabilistic network

The conditional probability structure reduces to the unconditional probability (UP) if the variable does not have a parent node. These probabilities (i.e., unconditional or

conditional probabilities) are evaluated from historical data, expert judgment, or their combination (Abogrean and Latif 2012; Cockburn and Tesfamariam 2012; Liu et al. 2011). When it comes to computation of probabilities of rare events in complex structural and infra-structure systems, Straub and Der Kiureghian (2010a; b) proposed a new method which combines BBN and structural reliability methods (SRMs). In a BBN analysis, for *n* number of mutually exclusive hypotheses $H_{i(i=1,\ldots\ldots,n)}$, and a given evidence E, the updated probability is computed by,

$$P(H_j|E) = \frac{p(E|H_j) \times p(H_j)}{\sum_{i=1}^{n} p(E|H_i) \times p(H_i)} \quad \textbf{2.1}$$

which states that the belief for a hypothesis $H_{j(j=1,\ldots,n)}$ upon obtaining evidence E can be computed by multiplying our previous belief $P(H_j)$ by the likelihood $P(E|H_j)$ that E will materialize if H_j is true. $P(H_j|E)$ is sometimes called the posterior probability (or simply *posterior*), and $P(H_j)$ is called the prior probability (or *prior*).

The advantages of use of BBN are, it can be established according to historical data, expert judgment, or their combination, and can be used to update probabilities when new information is available (Liu et al. 2011; McCann et al. 2006; Uusitalo 2007). New information includes evidence on one or more variables, or observed states that can be entered into the BBN. The new updated information propagates throughout the network to provide up-to-date probabilistic values.

Chapter 3: Proposed Bayesian Belief Network

This chapter demonstrates a seismic risk assessment framework using the Bayesian belief network (BBN) for high-voltage transformers in a substation. Although there are other reasons which are responsible for transformer vulnerability (e.g., deterioration of structural anchors, aging of transformer parts, etc.), this thesis only considers the vulnerability of high-voltage transformers due to seismic vibration. The beginning section gives a general ideal about the framework and subsequently, the framework is elaborated upon in the following sections. In the end, a sensitivity analysis is performed to investigate the significance of input parameters to the output result (i.e., transformer damage probability).

A Bayesian belief network (BBN) was used to evaluate the performance of the transformer in the event of an earthquake. In this thesis the nodes (i.e., variables) in BBN represent the performance of different components of a transformer and consequences induced by earthquake shaking. The links between them indicate informational or causal dependencies among the variables. To develop the risk assessment framework using BBN, the seismic performance of substation components was reviewed from past earthquake records (ASCE 1999; Eidinger and Tang forthcoming; Mitchell et al. 1990; Schiff 1997). Cause and effect analysis of the transformer vulnerability based on the past earthquake records showed that transformer damage is initiated due to soil instability, rocking response and interaction coming from the conductors, due to relative movement of the substation components.

Based on the cause and effect analysis of transformer vulnerability, a conceptual framework for transformer vulnerability was developed as shown in Figure 3.1. Figure 3.1

shows interaction coming from the conductors (IC), soil instability, and rocking response of transformer (RT) as a function of ground motion intensity measure. Finally, transformer vulnerability is related to earthquake induced objects (e.g., IC, soil instability, RT). This thesis denoted ground motion intensity measure, IC, soil instability, RC and transformer vulnerability as the objects of BBN. An object in a BBN framework is a distinct node behind which another BBN resides. When several variables are introduced to a BBN network, use of these objects reduces graphical clutter (Bensi et al. 2009). Thus, objects are introduced to proposed BBN framework to perform risk assessment of high-voltage transformer (Figure 3.1). The complete BBN framework with each of the BBN of these objects is shown in Figure 3.2 and elaborated in the following subsections and each of the BBN of the objects is described in the following subsections.

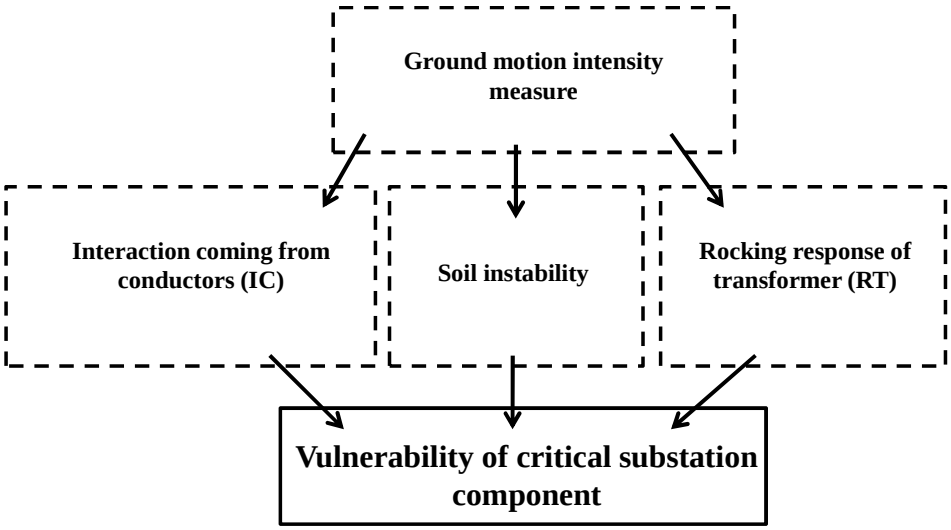

Figure 3.1 Conceptual BBN for high-voltage transformers

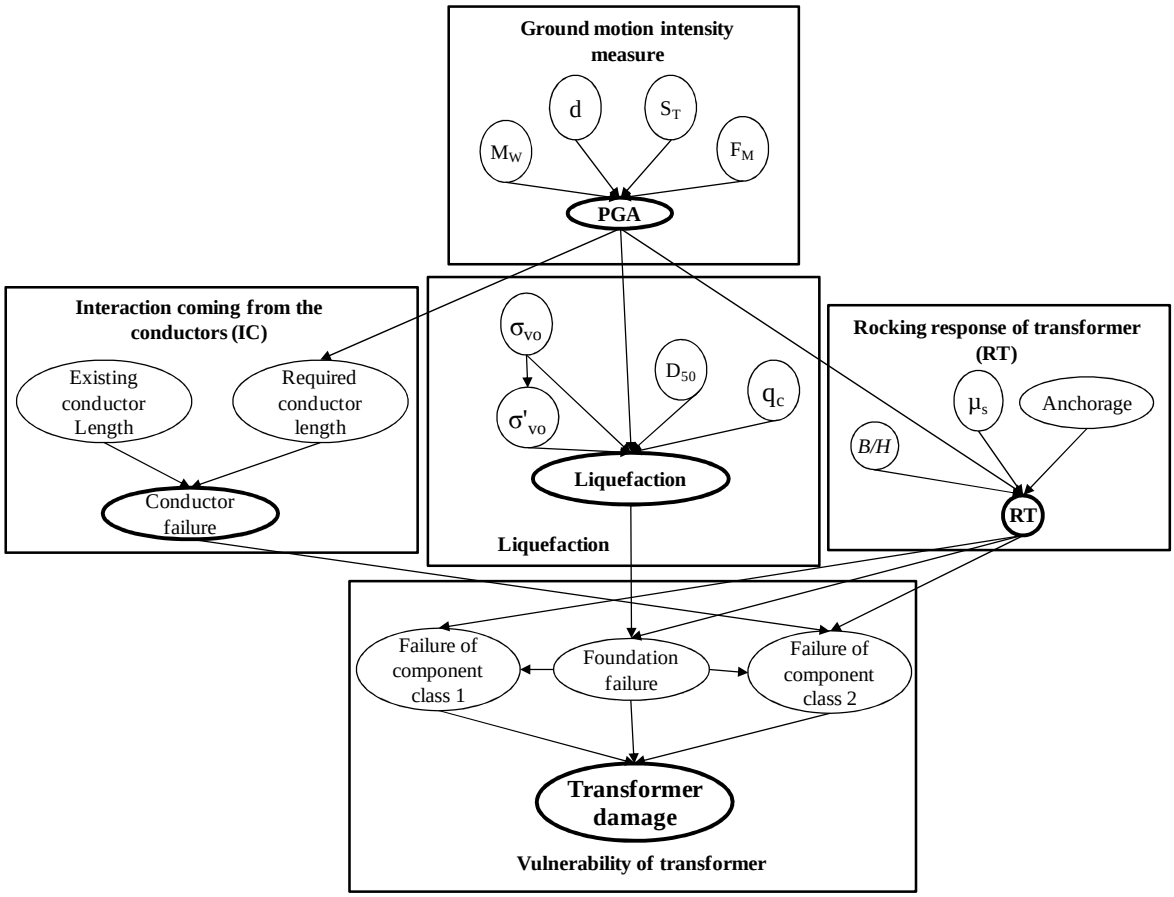

Figure 3.2 Proposed BBN for seismic risk assessment of transformer

3.1 Ground motion intensity measure

Ground motion is characterized by an intensity measure, which could be any one of a number of ground motion parameters (e.g., peak ground acceleration (PGA), spectral horizontal acceleration at a particular period) (Baker 2008). Several attenuation relationships are available to quantify ground motion intensity for several tectonic regions, such as western North America (Abrahamson and Silva 1997; Boore et al. 1997; Campbell 1997; Sadigh et al. 1997), eastern and central North America (Atkinson and Boore 1995; Toro et al. 1997), Cascadia subduction zone (Atkinson and Boore 1997; Youngs et al. 1997), etc. These models anticipate the probability distribution of ground motion intensity, as a function of different

variables such as the earthquake's magnitude, distance, faulting mechanism, the near-surface site conditions, the potential presence of directivity effects, etc (Baker 2008). Kuehn et al. (2009) used BBN for modeling dependencies between ground motion intensity and source/site characteristics. In their study, the BBN was developed based on the data available in PEER NGA database (PEER 2005). Later on Bensi et al. (2011) proposed another BBN model for modeling seismic demands, addressing all the shortcomings found in the previous studies of Bayraktarli et al. (2005, 2006) and Kuehn et al. (2009).

For this thesis, PGA was used as a ground motion intensity measure. To calculate PGA values, the attenuation equation provided by Boore et al. (1997) was used. Other studies on ground motion intensity measure could be used here, as well. Depending on the researcher's preference, an appropriate method should be selected. In their study ground motion intensity (i.e., spectral acceleration, horizontal peak ground acceleration) was given as a function of moment magnitude (M_w), site to fault distance (d), fault type, and soil type. Their model is valid if site to fault distance is in between 0-80km only and the moment magnitude range is in between 5.5 to 7.5. In their study, the faulting mechanism is defined into three types: strike-slip faulting, reverse-slip faulting and unknown faulting. For an unknown fault type the attenuation equation can be represented as follows,

$$\ln PGA = -0.242 + 0.527(M_w - 6) - 0.778 \ln R - 0.371 \ln(V_{s30}/1396) \quad \textbf{3.1}$$

where, $R = \sqrt{d^2 + 31.025}$ and V_{s30} is shear wave velocity of soil. Therefore, Figure 3.2 shows the ground motion intensity (i.e., horizontal PGA) as a function of moment magnitude (M_w), site to fault distance (d), soil type (S_T), and fault mechanism (F_M).

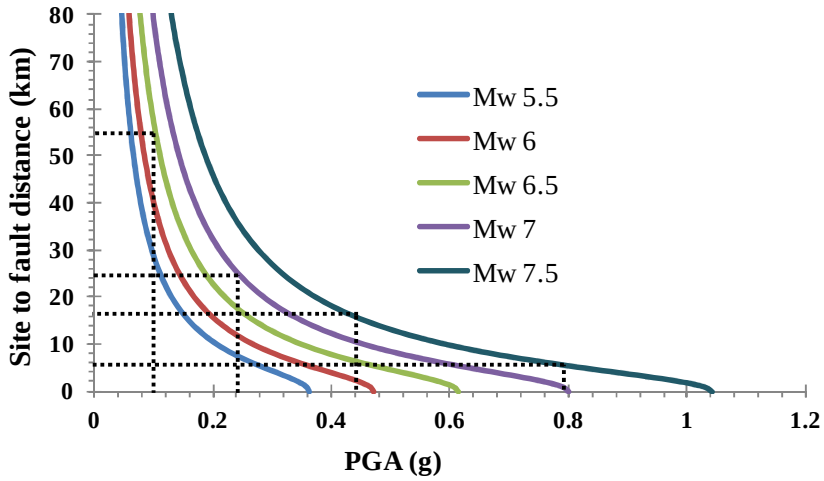

Figure 3.3 Attenuation of PGA as a function of site to fault distance (for soil type: NEHRP class E)

In this thesis, eight node states were used to describe PGA, namely, extremely extremely low (EEL_{PGA}), extremely low (EL_{PGA}), very low (VL_{PGA}), low (L_{PGA}), medium (M_{PGA}), high (H_{PGA}), very high (VH_{PGA}), and extremely high (EH_{PGA}); corresponding PGA range of each node states are 0≤ PGA <0.10, 0.10≤ PGA <0.15, 0.15≤ PGA <0.20, 0.20≤ PGA <0.30, 0.30≤ PGA <0.40, 0.40≤ PGA <0.60, 0.60≤ PGA <0.80, and 0.80≤ PGA <1.0, respectively. Five node states, with different range of d (d_{0-5}, d_{5-15}, d_{15-25}, d_{25-55}, and d_{55-80}) were also defined to describe site to fault distance (d). Selection of range of values, corresponding to each node state of d was done following Figure 3.3. For example, when PGA ranges from 0.8 to 1g, d varies from 0 to 5km (which is representing very low value). Table 3.1 shows the node states and corresponding values of input variable.

Table 3.1 Description of basic input parameters for "ground motion intensity measure"

Variable (Unit)	States	Value	UP
$\mathbf{M_W}$	$M_{5.5}$	$M_W = 5.5$	0.20
	$M_{6.0}$	$M_W = 6$	0.20
	$M_{6.5}$	$M_W = 6.5$	0.20
	$M_{7.0}$	$M_W = 7$	0.20
	$M_{7.5}$	$M_W = 7.5$	0.20
d (km)	$d_{0\text{-}5}$	$0 \leq d < 5$	0.20
	$d_{5\text{-}15}$	$5 \leq d < 15$	0.20
	$d_{15\text{-}25}$	$15 \leq d < 25$	0.20
	$d_{25\text{-}55}$	$25 \leq d < 55$	0.20
	$d_{55\text{-}80}$	$55 \leq d < 80$	0.20
S_T (V_{s30} in m/sec)	Class A	V_{s30}=1890	0.20
	Class B	V_{s30}=1070	0.20
	Class C	V_{s30}=520	0.20
	Class D	V_{s30}=250	0.20
	Class E	V_{s30}=150	0.20

Furthermore, moment magnitude (M_W) was discretized into 5.5, 6, 6.5, 7, and 7.5; the corresponding states were named as $M_{5.5}$, $M_{6.0}$, $M_{6.5}$, M_7, and $M_{7.5}$, respectively. Soil type (S_T) was discretized into five states based on the shear wave velocity of soil (V_{s30}), similar to NEHRP site classes[2] (i.e., class A, class B, class C, class D, and class E). The classification of soil type is described more elaborately in Appendix A. Finally, fault mechanism (F_M) was considered to be fixed (i.e., unknown faulting). The unconditional probability (UP) table corresponds to each states of input parameters are also shown in Table 3.1. The UPs of M_w, d and S_T were defined as $1/n = 1/5 = 0.20$ (Cockburn and Tesfamariam 2012).

Table 3.2 shows the conditional probabilities for node variable PGA. To develop the CPT table, 124 pairs of M_W ($M_{5.5}$, $M_{6.0}$, $M_{6.5}$, M_7, $M_{7.5}$), d (d_{0-5}, d_{5-15}, d_{15-25}, d_{25-55},

[2] Weblink: *http://www.seis.utah.edu/urban/nehrp.shtml* (Last visited February 11, 2013)

d_{55-80}), and S_T (class A, class B, class C, class D, class E) were selected and the median PGA values were calculated using the Equation 3.1. Here, the subscript in the states denotes the range of values or discrete values to the corresponding state. Finally, the calculated values of PGA along with the UP of input variables were synthesized into Netica software (Norsys Software Corp 2006) to develop the CPT. A snapshot of these probabilities is shown in Table 3.2.

Table 3.2 Snapshot of the CPT for node variable "PGA"

	PGA
(M_W, d, S_T)	**(EL_{PGA},VL_{PGA}, L_{PGA}, M_{PGA}, H_{PGA}, VH_{PGA}, EH_{PGA}, EEH_{PGA})**
($M_{5.5}$, $d_{0\text{-}5}$, Class A)	(0.144, 99.017, 0.137, 0.136, 0.144, 0.132, 0.149, 0.141)
($M_{6.0}$, $d_{0\text{-}5}$, Class E)	(0.174, 0.161, 0.169, 0.177, 0.158, 98.836, 0.158, 0.165)
……	……
……	……
($M_{5.5}$, $d_{15\text{-}25}$, Class A)	(98.749, 0.169, 0.175, 0.184, 0.179, 0.188, 0.188, 0.169)
($M_{6.0}$, $d_{15\text{-}25}$, Class E)	(0.183, 0.181, 98.716, 0.190, 0.181, 0.188, 0.179, 0.182)
……	……
……	……
($M_{5.5}$, $d_{55\text{-}80}$, Class A)	(98.756, 0.187, 0.169, 0.164, 0.177, 0.186, 0.182, 0.178)
($M_{7.5}$, $d_{55\text{-}80}$, Class A)	(99.005, 0.147, 0.141, 0.141, 0.137, 0.148, 0.135, 0.145)

3.2 Soil instability

Soil instability is one of the factors that may trigger by ground vibration and may cause the failure of substation components (ASCE 1999; Eidinger and Tang forthcoming). This thesis considered only soil instability due to liquefaction. Several studies have been performed so far to predict the liquefaction initiation in the event of an earthquake. These studies quantified the soil liquefaction using deterministic and probabilistic techniques, which is either based on laboratory tests or empirical correlations. The deterministic empirical correlation proposed by Seed and Idriss (1971) using Standard Penetration Test

(SPT) is a widely used method in practice. Later on their method was revised by Youd et al. (2001). On the other hand, Bayraktarli (2006), Cetin et al. (2002), Tesfamariam and Liu (2013), etc. used a Bayesian framework for probabilistic assessment of the initiation of seismic soil liquefaction. For this thesis, BBN framework for predicting liquefaction initiation was adapted from Tesfamariam and Liu (2013) (Figure 3.2). Other studies on predicting liquefaction initiation could be used here, as well. Depending on the researcher's preference, an appropriate method should be selected.

In this thesis, liquefaction was conditioned on five factors, PGA, average grain size (D_{50}), CPT tip resistance (q_c), total vertical over-burden pressure (σ_{vo}) and effective vertical overburden pressure (σ'_{vo}). Effective vertical overburden pressure (σ'_{vo}) was conditioned on total vertical over-burden pressure (σ_{vo}). This thesis used the historical data available in the literature Timothy and Scott (1995) to predict the liquefaction initiation. The highest value of PGA in the database was found 0.6g. To capture the effect of PGA from 0.6g to 1g, a very high liquefaction initiation probability was assumed with a PGA of 0.6g to 1g. As liquefaction initiation requires local ground acceleration greater than 0.10g (Morales and Morales 2003), it was assumed that liquefaction would not occur between a PGA range of 0 to 0.1g.

Table 3.3 shows the node states of all the input variables used in the liquefaction prediction.

Table 3.3 Description of basic input parameters for "soil instability"

Variable (Unit)	States	Value	UP
PGA (g)	Extremely Low (EL)	$0 \leq PGA < 0.10$	-
	Very Low (VL)	$0.10 \leq PGA < 0.15$	-
	Low (L)	$0.15 \leq PGA < 0.20$	-
	Medium (M)	$0.20 \leq PGA < 0.30$	-
	High (H)	$0.30 \leq PGA < 0.40$	-
	Very High (VH)	$0.40 \leq PGA < 0.60$	-
	Extremely High (EH)	$0.60 \leq PGA < 0.80$	-
	Extremely Extremely High (EEH)	$0.80 \leq PGA < 1.0$	-
D_{50} (mm)	Very Low ($VL_{0\text{-}0.05}$)	$0 \leq D_{50} < 0.05$	0.591
	Low ($L_{0.05\text{-}0.10}$)	$0.05 \leq D_{50} < 0.10$	0.283
	Medium ($M_{0.10\text{-}0.15}$)	$0.10 \leq D_{50} < 0.15$	0.157
	High ($H_{0.15\text{-}0.30}$)	$0.15 \leq D_{50} < 0.30$	0.300
	Very High ($VH_{0.30\text{-}0.60}$)	$0.30 \leq D_{50} < 0.60$	0.201
q_c (MPa)	Very Low ($VL_{0\text{-}1.5}$)	$0 \leq q_c < 1.5$	0.140
	Low ($L_{1.5\text{-}3}$)	$1.5 \leq q_c < 3$	0.251
	Medium ($M_{3\text{-}6}$)	$3 \leq q_c < 6$	0.251
	High ($H_{6\text{-}12}$)	$6 \leq q_c < 12$	0.209
	Very High ($VH_{12\text{-}30}$)	$12 \leq q_c < 30$	0.149
σ_{vo} (KPa)	Very Low ($VL_{0\text{-}50}$)	$0 \leq \sigma_{vo} < 50$	0.135
	Low ($L_{50\text{-}70}$)	$50 \leq \sigma_{vo} < 70$	0.203
	Medium ($M_{70\text{-}100}$)	$70 \leq \sigma_{vo} < 100$	0.228
	High ($H_{100\text{-}150}$)	$100 \leq \sigma_{vo} < 150$	0.243
	Very High ($VH_{150\text{-}300}$)	$150 \leq \sigma_{vo} < 300$	0.190
σ'_{vo} (KPa)	Very Low ($VL_{0\text{-}40}$)	$0 \leq \sigma'_{vo} < 40$	-
	Low ($L_{40\text{-}60}$)	$40 \leq \sigma'_{vo} < 60$	-
	Medium ($M_{60\text{-}100}$)	$60 \leq \sigma'_{vo} < 100$	-
	High ($H_{100\text{-}150}$)	$100 \leq \sigma'_{vo} < 150$	-
	Very High ($VH_{150\text{-}250}$)	$150 \leq \sigma'_{vo} < 250$	-

*Note: The subscript denotes the range of values for each state

In this thesis, PGA was discretized into eight states (as discussed in the previous section). The range of values of PGA (see Table 3.3) for each node states was selected according to Figure 3.4. Figure 3.4 shows that liquefaction initiation was observed when PGA values were more than 0.1g. PGA ranges from 0.1 to 0.3g shows a significant amount of data points for liquefaction initiation; therefore, more discretization (i.e., very low, low,

medium) was made for this range of PGA. After 0.3g, PGA values were discretized uniformly.

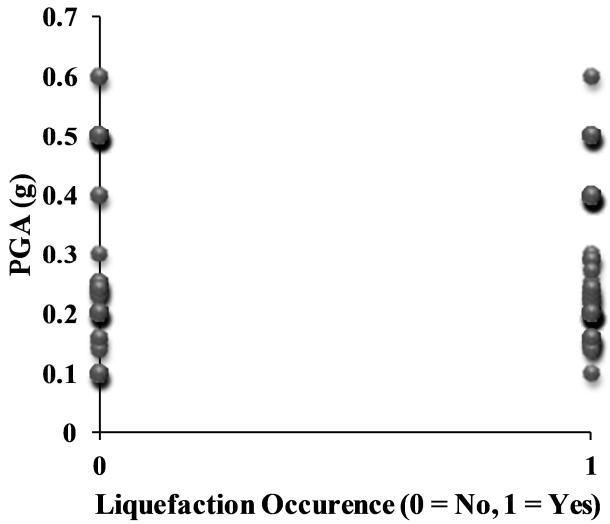

Figure 3.4 PGA vs. liquefaction occurrence (based on the historical data provided in Timothy and Scott (1995))

Five node states very low, low, medium, high, very high were also defined to describe D_{50}, q_c, σ_{vo}, and σ'_{vo}. Finally, liquefaction was considered to have two states, liquefaction occurrence ("Yes") and non-occurrence ("No"). The range of values of each node state for all the variables is given in Table 3.3. Based on the available historical data (Timothy and Scott 1995) liquefaction occurrence versus, σ_{vo}, σ'_{vo}, D_{50}, and q_c bar charts were plotted in Figure 3.5.The graphs show the relation between liquefaction occurrence and the variables. Finally, all the data were synthesized into Netica software (Norsys Software Corp 2006) to develop the CPT. A snapshot of these probabilities are shown in Table 3.3.

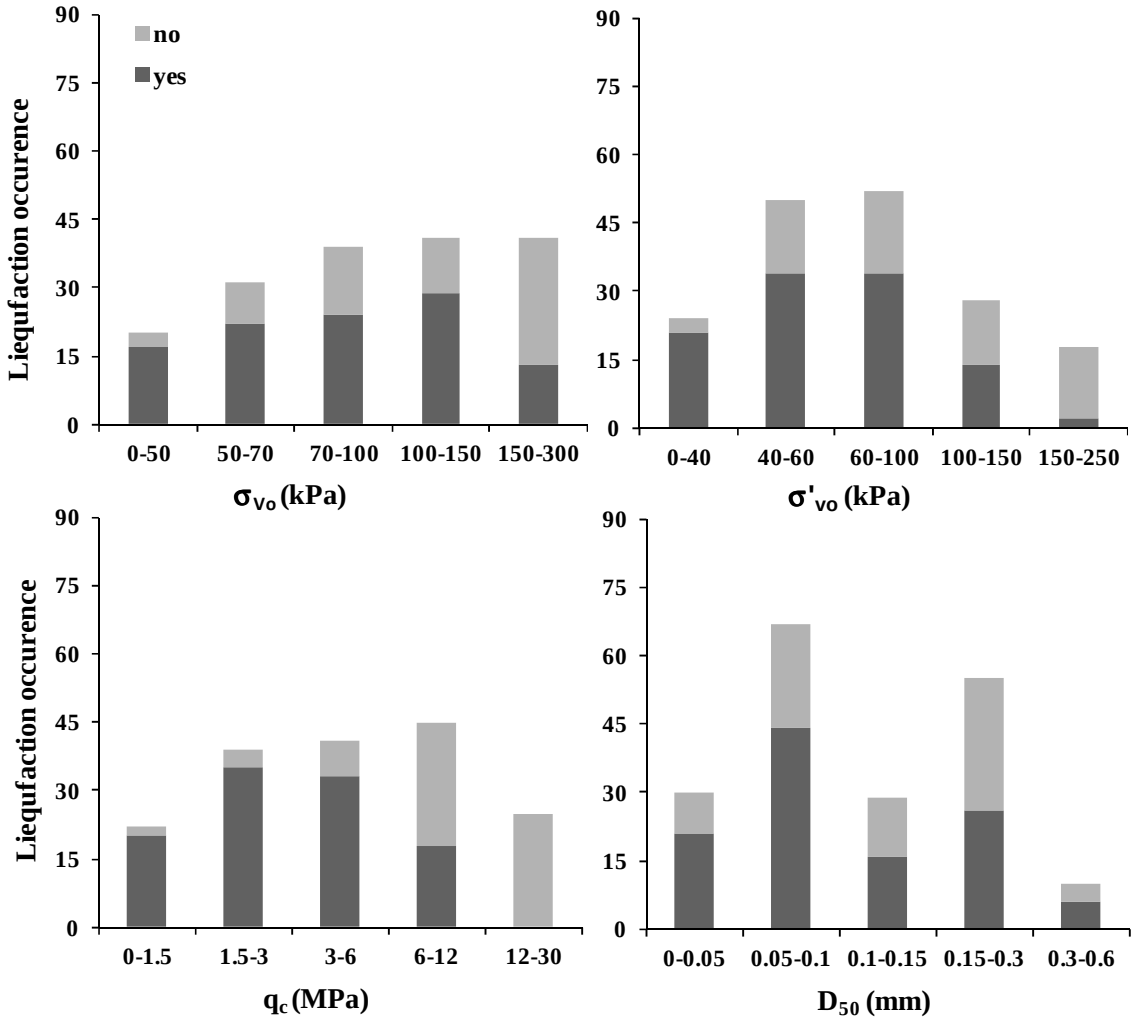

Figure 3.5 Liquefaction occurrence versus σ_{vo}, σ'_{vo}, q_c, and D_{50}

Table 3.4 Snapshot of the CPT for node variable "liquefaction"

(PGA, D_{50}, q_c, σ_{vo}, σ'_{vo})	**Liquefaction (Yes, No)**
(Extremely Low, $VL_{0\text{-}0.05}$, $VL_{0\text{-}1.5}$, $VL_{0\text{-}50}$, $VL_{0\text{-}40}$)	(0.002, 99.998)
(Medium, $VL_{0\text{-}0.05}$, $VH_{12\text{-}30}$, $VL_{0\text{-}50}$, $L_{40\text{-}60}$)	(44.023, 55.977)
……	……
……	……
(Very High, $L_{0.05\text{-}0.10}$, $VL_{0\text{-}1.5}$, $H_{100\text{-}150}$, $M_{60\text{-}100}$)	(53.650, 46.350)
(High, $H_{0.15\text{-}0.30}$, $H_{6\text{-}12}$, $L_{50\text{-}70}$, $VL_{0\text{-}40}$)	(48.465, 51.535)
……	……
……	……
(Extremely High, $VH_{0.30\text{-}0.60}$, $M_{3\text{-}6}$, $M_{70\text{-}100}$, $VH_{150\text{-}250}$)	(99.998, 0.002)
(Extremely High, $H_{0.15\text{-}0.30}$, $H_{6\text{-}12}$, $L_{50\text{-}70}$, $L_{40\text{-}60}$)	(99.998, 0.002)

3.3 Interaction coming from the conductors

The conductor connection flexibility between substation equipment affects earthquake equipment damage (ASCE 1999). Substation equipment may experience significant displacement at interconnected points (as shown in Figure 3.6), that may lead to conductor failure between the interconnected components. Der Kiureghian et al. (1999a) investigated the effect of interaction between the substation equipment interconnected by different type of conductors (i.e., rigid conductor and flexible conductor). They found that the seismic responses of cable connected equipment were significantly higher if compared with stand-alone equipment. Later on in Der Kiureghian et al. (1999b), they extended their previous work by doing further investigation on different conductor types. In addition to that Der Kiureghian et al. (2001) investigated the behavior of equipment connected with spring-dashpot-mass elements representing a conductor bus, Song et al. (2007) investigated the behavior of equipment connected with non-linear rigid bus conductor, and Hong et al. (2001) investigated the behavior of equipment connected with cable conductor and the influence of different parameters of cable conductors on the response of connected equipment.

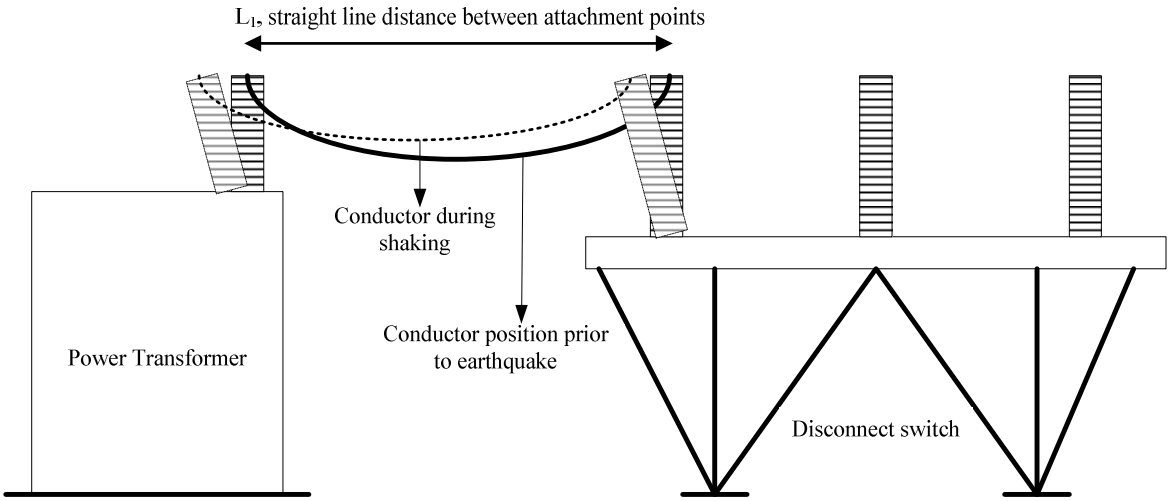

Figure 3.6 Behaviour of cable connected equipments (power transformer and disconnect switch) during an earthquake event

Dastous et al. (2004) proposed a simple method to estimate expected displacement of the substation equipment under seismic excitation. Methodology proposed by Dastous et al. (2004) to calculate the displacement of the substation components used generalized SDOF method. The process to estimate the required slack between the equipment is reported in detail in IEEE-1527 (2006) and IEEE-693 (2005). The conductor failure will occur if sufficient slack has not been provided in the conductor between the moving components (Der Kiureghian et al. 1999a). The first step to estimate the displacement between interconnected equipment would be an estimation of individual displacement of the equipment. Once the displacement is known, it is possible to compare the required slack (based on calculated displacements) with the provided slack, to find out whether there would be any conductor failure or not.

Following IEEE-693 (2005), the expected deflections for different voltage equipment (hence different natural frequencies), are provided in ASCE (1999) and the values are shown in Table 3.5.

Table 3.5 Typical equipment displacement (ASCE 1999)

Frequency	Operating Voltage		
	138kV	**230kV**	**500kV**
High : 8 Hz and greater: transformer, tank reactor, dead tank circuit breakers	25-50mm	25-75mm	100-300mm
Medium : 2.5-8Hz: disconnect switches, live-tank circuit breakers, capacitor banks	50-150mm	200-1000mm	300-1500mm
Low : under 2.5Hz: capacitor voltage transformers, current transformers, wave traps, suspended components	150-500mm	200-1000mm	300-1500mm

The conductor length between two adjacent items of equipment should be enough to accommodate the relative displacement between the equipment. This relative displacement can be evaluated using the square root of the sum of the squares (SRSS), absolute sum method and combine displacements using the complete quadratic combination (CQC) (for more detail calculation see IEEE-693 (2005)). Equation 3.2 shows the calculation of relative displacement using SRSS method (IEEE-1527 2006).

$$D_{rel} = 1.25 \times \sqrt{x_{max,1}^2 + x_{max,2}^2} \quad \textbf{3.2}$$

where, D_{rel} is the maximum horizontal relative displacement between equipment 1 and 2, $x_{max,1}$ is the maximum standalone displacement of equipment 1 in the conductor direction, and $x_{max,2}$ is the maximum standalone displacement of equipment 2 in the conductor direction. Using Equation 3.2, the relative displacement between transformer and disconnect switch (the adjacent equipment to power transformer) can be calculated. The calculated D_{rel} values are shown in Table 3.6.

Table 3.6 Calculated relative displacements between transformer and disconnect switch

Description	Operating Voltage		
	138kV	**230kV**	**500kV**
Relative displacement between power transformer and disconnect switch	70-198mm	93-267mm	280-839mm

The required conductor length between interconnected components can be estimated using the following equation.

$$L_o = L_1 + L_2 + D_{rel} \quad \textbf{3.3}$$

where, the L_1 is the length of the straight line distance between attachment points (see Figure 3.6) and L_2 is an additional provision for the conductor configuration under consideration, as to not transfer unnecessary additional loads to the equipment when fully stretched. Here, sum of L_1 and L_2 will give a constant value, hence, D_{rel} in the equation will basically determine whether the conductor length is adequate to withstand a seismic event or not.

The conductor failure can be determined by comparing the existing conductor length and the required conductor length. Figure 3.2 shows that the conductor failure is a function of existing conductor length (ECL) and required conductor length (RCL), and the required conductor length is conditioned on seismic hazard (i.e., PGA). When PGA is high, the required conductor length is high and vice versa. In this thesis, conductor failure was discretized into three states, namely, unlikely (UL_{CF}), likely (L_{CF}) and very likely (VL_{CF}). Furthermore, five node states corresponds to very low (VL_{1-150}), low ($L_{150-300}$), medium ($M_{300-450}$), high ($H_{450-700}$), and very high ($VL_{700-1000}$) were also defined to describe existing conductor length (ECL) and required conductor length (RCL). Here, the subscript in

each of the state denotes the range of values for the corresponding states, which is provided in Table 3.7.

Table 3.7 Description of basic input parameters for IC: existing conductor length (ECL)/ required conductor length (RCL)

Operating voltage of equipment	States	Value of conductor length (CL), (mm)	UP for ECL
138kV	Very low	1≤ CL <50	0.20
	Low	50≤ CL <100	0.20
	Medium	100≤ CL <150	0.20
	High	150≤ CL <200	0.20
	Very high	200≤ CL <250	0.20
230kV	Very low	1≤ CL <75	0.20
	Low	75≤ CL <150	0.20
	Medium	150≤ CL <225	0.20
	High	225≤ CL <300	0.20
	Very high	300≤ CL <375	0.20
500kV	Very low	1≤ CL <150	0.20
	Low	150≤ CL <300	0.20
	Medium	300≤ CL <450	0.20
	High	450≤ CL <700	0.20
	Very high	700≤ CL <1000	0.20

The range of values corresponds to each states were assumed based on Table 3.6. As mentioned before, the length of the conductor is a sum of a constant value (i.e., $L_1 + L_2$) and relative displacement, D_{rel}; the range of values for each state was assumed based on D_{rel} (i.e., ignoring the constant part). The corresponding unconditional probability of each parameter (i.e., ECL and RCL) was defined as $1/n$ (Cockburn and Tesfamariam 2012). Finally, with the consideration of two input parameters (i.e., ECL and RCL), the CPT for the "conductor failure" was generated. A snapshot of that CPT is shown in Table 3.8. The complete table is given in Appendix B. It is a knowledge based conditional probability table. For example, when (ECL, RCL) is ($L_{150-300}$, $M_{300-450}$), the probability of conductor failure will be high; corresponding conditional probabilities of conductor failure (UL_{CF}, L_{CF}, VL_{CF})

were assumed (5, 30, 65) (Table 3.8). Conversely, when the (ECL, RCL) is ($M_{300-450}$, $L_{150-300}$), the probability of conductor failure will be low; corresponding conditional probabilities of conductor failure (UL_{CF}, L_{CF}, VL_{CF}) were assumed (80, 15, 5) (Table 3.8). The basis of this assumption is, when existing conductor length is lower than the required, the conductor failure is very likely and vice versa.

Table 3.8 Snapshot of the CPT for node variable "conductor failure"

(ECL, RCL)	**Conductor failure (UL_{CF}, L_{CF}, VL_{CF})**
($VL_{1\text{-}150}$, $VL_{1\text{-}150}$)	(80, 20, 0)
($L_{150\text{-}300}$, $M_{300\text{-}450}$)	(5, 30, 65)
……	……
……	……
($M_{300\text{-}450}$, $L_{150\text{-}300}$)	(80, 15, 5)
($M_{300\text{-}450}$, $H_{450\text{-}700}$)	(25, 30, 45)
……	……
……	……
($VH_{700\text{-}1000}$, $H_{450\text{-}700}$)	(75, 20, 5)
($VH_{700\text{-}1000}$, $VH_{700\text{-}1000}$)	(60, 30, 10)

3.4 Rocking response of transformers

Several cases have been found, by searching the past earthquake records, that the transformer moved back and forth. Some of the records showed that due to back and forth movement of the transformer, the foundation tilted and remained tilted after the earthquake. In some cases, the foundation remained in its position, but damage to bus work indicated that there was a back and forth movement during the earthquake (ASCE 1999). Makris and Roussos (1998, 2000) investigated the rocking response of free standing block and Makris and Zhang (1999, 2001) investigated the rocking response of anchored blocks. The free standing transformer will experience the rocking response without experiencing any restoring

force coming from the anchorage. On the other hand, the anchored transformer will not rock until the strength of the restrainer has exceeded its fracture. Makris and Black (2002) investigated the uplifting and overturning of equipment anchored to a base foundation. Their study looked into the performance of high strength restrainer for a wide range of earthquake motion. This thesis considered both the rocking response of free standing transformers and anchored transformers.

Strong ground motion may initiate slide or set up a rocking motion to electrical transformers that may result in substantial damage. Shenton (1996) derived the governing criteria of the initiation of the slide and rock modes from rest for a rigid, rectangular block (i.e., transformer) subjected to horizontal foundation acceleration. The governing equations for rest, slide, and rock modes for a rectangular free standing rigid block are presented in Table 3.9.

Table 3.9 Governing conditions for rest, slide, and rock modes

Modes	Conditions
Rest	$PGA \leq \mu_s$; and $PGA \leq B/H$
Slide	$\mu_s \leq PGA$; and $B/H \leq \mu_s$
Rock	$B/H < PGA$; and $B/H < \mu_s$

*Note: A_g = PGA, peak ground acceleration, B/H= width to height ratio of a rigid block, μ_s=Static coefficients of friction

These criteria were plotted in the μ_s, versus PGA parameter space for a block with a width to height ratio (e.g., B/H) of 0.50 as shown in Figure 3.7. The parameter space is divided into three regions by the lines corresponding to $\mu_s = PGA$, $\mu_s = B/H = 0.5$, and $PGA = B/H = 0.5$. These three regions correspond to rest, slide, and rock.

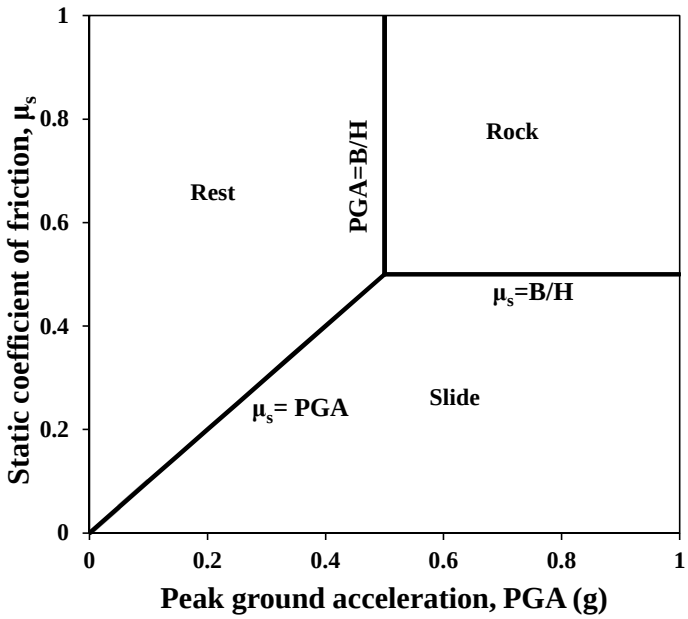

Figure 3.7 Boundaries of rest, slide, and rock modes, for H/B=2 (based on Shenton (1996))

Therefore, the rocking response of a transformer depends on four factors, anchorage, PGA, static coefficients of friction (μ_s), and width to height ratio (B/H) (Figure 3.2). This thesis considered that, if the transformer were unanchored, the rocking response would follow the criteria provided by Shenton (1996) and that if the transformer were anchored, it would not rock until the anchorage failed. Hence, the variable "anchorage" has two states, anchored and unanchored. In this thesis, RT assumed to have three states, rest, slide, and rock. Furthermore, B/H ratio had eight states, $A_{0.34}$, $B_{0.39}$, $C_{0.42}$, $D_{0.43}$, $E_{0.50}$, $F_{0.51}$, $G_{0.65}$ and $H_{0.69}$. Here, the subscripts denote the value of B/H. Each of the state denotes width to height ratio (B/H) of transformers given in Makris and Roussos (1998). μ_s had only one state, representing the coefficient of friction between the concrete (the base at which the transformer is resting) and steel (material of the transformer bottom). The value of the coefficient of friction between concrete and steel is 0.45. The range of values that

corresponds to each state of the input parameters is shown in Table 3.10. The corresponding UP of each parameter was calculated as $1/n$ (as previous).

Table 3.10 Description of basic input parameters for "Rocking response of transformer"

Variable	States	Value	UP
PGA	Extremely Low	0≤ PGA <0.10	-
	Very Low	0.10≤ PGA <0.15	-
	Low	0.15≤ PGA <0.20	-
	Medium	0.20≤ PGA <0.30	-
	High	0.30≤ PGA <0.40	-
	Very High	0.40≤ PGA <0.60	-
	Extremely High	0.60≤ PGA <0.80	-
	Extremely Extremely High	0.80≤ PGA <1.0	-
B/H	$A_{0.34}$	0.34	0.125
	$B_{0.39}$	0.39	0.125
	$C_{0.42}$	0.42	0.125
	$D_{0.43}$	0.43	0.125
	$E_{0.50}$	0.50	0.125
	$F_{0.51}$	0.51	0.125
	$G_{0.65}$	0.65	0.125
	$H_{0.69}$	0.69	0.125
Anchorage	Anchored	-	0.50
	Unanchored	-	0.50

Table 3.11 shows the snapshot of CPT for the node variable RT. The complete table is provided in Appendix C for the anchored transformer. The probabilities for an unanchored transformer were calculated based on the governing conditions provided by Shenton (1996) (see Table 3.9). While calculating the probabilities, it was assumed that 100% probability of being at rest, slide and rock mode would be considered when the combination of PGA and B/H values fell in the 'ash colored zone' (marked in the Figure 3.8). When the points fell outside the marked zone, the assumption was that the probability of being in that specific zone would be decreased linearly. For example, if a point was just outside the line connecting points 1 and 2, the probability of being at rest would not be 100%; there would be some

probabilities of being at slide mode. If the point moved towards the line $\mu_s = PGA$, probability of being at rest would be decreased linearly; if the point was on the line, the probability of being at rest and slide would be equal. If the transformer was anchored, the probabilities were assigned based on some assumptions, such as the transformer would be at rest for low PGA values and the probability of transformer being at rocking and sliding mode would increase with the increment of PGA (as high PGA may fracture the anchorage). For example, Table 3.11 shows, when the input (PGA, B/H, Anchorage, μ_s) is (Extremely High, $A_{0.34}$, Unanchored, 0.45), the probabilities of being at rest, slide and rock mode are (0, 17.25, 82.75). On the other hand, when the input is (Extremely High, $A_{0.34}$, Anchored, 0.45,), the probability of fracturing of anchorage is high (as PGA is high), as the output shows (Rest, Slide, Rock) = (43, 12, 45).

Table 3.11 Snapshot of the CPT for node variable "RT"

(PGA, B/H, Anchorage, μ_s)	**RT (Rest, Slide, Rock)**
(Extremly Low, $A_{0.34}$, Anchored, 0.45)	(100, 0, 0)
(Low, $F_{0.51}$, Unanchored, 0.45)	(100, 0, 0)
……	……
……	……
(Very High, $A_{0.34}$, Anchored, 0.45)	(48, 10, 42)
(Very High, $G_{0.65}$, Unanchored, 0.45)	(46.02, 49.09, 4.88)
……	……
……	……
(Extremly High, $A_{0.34}$, Anchored, 0.45)	(43, 12, 45)
(Extremly High, $A_{0.34}$, Unanchored, 0.45)	(0, 17.25, 82.75)

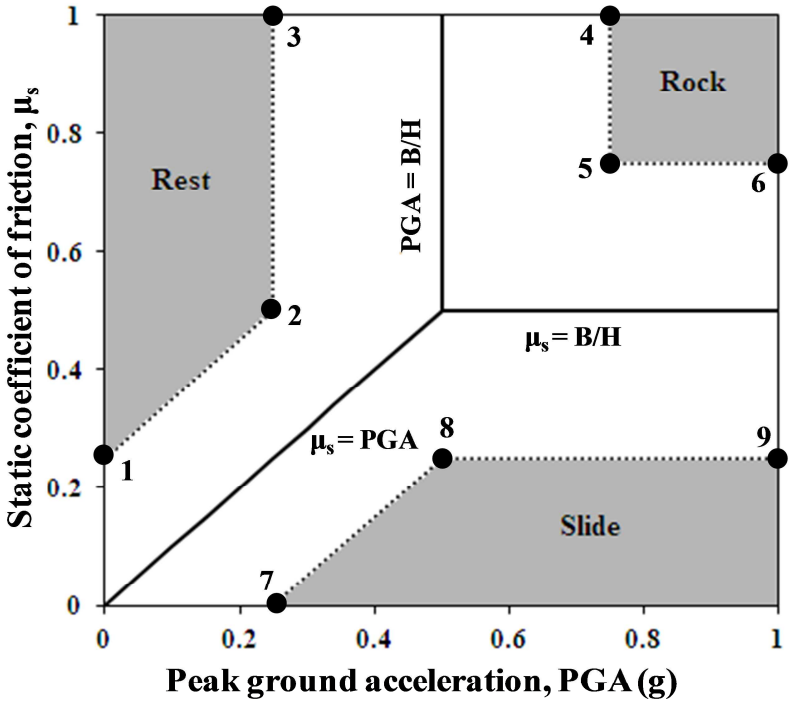

Co-ordinates of the points:
1 = [0.5 B/H, 0], **2** = [0.5 B/H, B/H], **3** = [0.5 B/H, 1], **4** = [0.5 (1+B/H), 1]
5 = [0.5 (1+B/H), 0.5 (1+B/H)], **6** =[1, 0.5 (1+B/H)], **7** =[0.5 B/H, 0]
8 = [B/H, 0.5 B/H], **9** = [1, 0.5 B/H]

Figure 3.8 Boundaries of rest, slide, and rock modes to calculate CPT

3.5 Transformer vulnerability

Based on past earthquake records, ASCE (1999) elaborated on the earthquake performance of power transformers. The causes of failure of transformer components during an earthquake are listed in Table 3.12. Table 3.12 shows that causes of failure of transformer components during an earthquake are considered to be due to conductor interaction between interconnected equipment, liquefaction and rocking response.

Table 3.12 Causes and effects of failure of transformer components

Component	Cause	Effect/Observed failure
Foundation failure	▪ Soil liquefaction/ differential settlement ▪ Rocking effect	▪ Tilt of a foundation ▪ Soil may remain level, but the due to back and forth movement other parts of the transformer may fail (e.g., low voltage bus, bushing, lightning arrester, radiators, conductor failure due to relative movement)
Radiator failure (less probable to fail)	▪ Relative movement of the transformer and the radiator (for self supported radiators).	▪ Oil leakage at the coupling ▪ For non-manifold radiators, the observed failure was found for a PGA 0.15g during Northridge EQ ▪ Deformation in the manifold support is found
Internal parts	▪ Earthquake induced vibration	▪ Internal transformer fault, which may trigger the circuit breaker to open
Conservator failure	▪ Relative movement of the conservator and the transformer case.	▪ The structural support system failed ▪ The pipe connection between the conservator and transformer tank failed ▪ A piping failure may result in an oil spill
Lightning arrester and tertiary bushing failure	▪ The flexibility of bus support structures imposed loads on the bushings	▪ Failure of lightning arrester and tertiary bushing
Porcelain bushing failure	▪ Inertial loads on bushings due to ground vibrations ▪ Rocking response of transformer ▪ Interaction loads from the conductors ▪ Effect of failed lightning arrester	▪ Failure of porcelain bushing

Based on the studied causes and effects of transformer component failure, a BBN for transformer vulnerability was developed (shown in Figure 3.2). In this thesis, the components were classified into two groups, component class 1 (i.e., radiator, internal parts, and conservator) and component class 2 (i.e., lightning arrester and tertiary bushing failure, porcelain bushing failure). The classification was done depending on the causes of failure. Components that fail due to the transformer rocking response and foundation failure were

named as component class 1 and components that fail due to conductor failure and transformer rocking response, and foundation failure were named as component class 2 (Table 3.12).

Hence, the foundation failure is conditioned on RT and liquefaction, component class 1 is conditioned on RT and foundation failure, and finally, component class 2 is conditioned on IC, RT and foundation failure. In the end, transformer damage is a function of foundation failure and component failure (classes 1 and 2). The foundation failure, the failure of component class 1, and the failure of component class 2 were considered to have two states, likely to fail and unlikely to fail. The variable transformer damage had three states, low, medium and high probability of damage. Table 3.13, Table 3.14, Table 3.15, and Table 3.16 show the CPT for foundation failure, failure of component class 1, failure of component class 2, and transformer damage. These tables are knowledge based conditional probability table.

Table 3.13 Description of CPT for node variable "foundation failure"

(RT, Liquefaction)	**Foundation failure (Unikely, Likely)**
(Rest, Yes)	(30, 70)
(Rest, No)	(99, 1)
(Slide, Yes)	(5, 95)
(Slide, No)	(70, 30)
(Rock, Yes)	(1, 99)
(Rock, No)	(45, 55)

Table 3.14 Description of CPT for node variable "failure of component class 1"

(RT, Foundation failure)	**Failure of component class 1 (Unlikely, Likely)**
(Rest, Unlikely)	(99, 1)
(Rest, Likely)	(30, 70)
(Slide, Unlikely)	(40, 60)
(Slide, Likely)	(20, 80)
(Rock, Unlikely)	(30, 70)
(Rock, Likely)	(1, 99)

Table 3.15 Description of CPT for node variable "failure of component class 2"

(Conductor failure, RT, Foundation failure)	Failure of component class 2 (Likely, Unlikely)
(Unlikely, Rest, Unlikely)	(99, 1)
(Unlikely, Rest, Likely)	(40, 60)
(Unlikely, Slide, Unlikely)	(45, 55)
(Unlikely, Slide, Likely)	(30, 70)
(Unlikely, Rock, Unlikely)	(40, 60)
(Unlikely, Rock, Likely)	(20, 80)
(Likely, Rest, Unlikely)	(45, 55)
(Likely, Rest, Likely)	(25,75)
(Likely, Slide, Unlikely)	(35, 65)
(Likely, Slide, Likely)	(15, 85)
(Likely, Rock, Unlikely)	(20, 80)
(Likely, Rock, Likely)	(10, 90)
(Very Likely, Rest, Unlikely)	(35, 65)
(Very Likely, Rest, Likely)	(15, 85)
(Very Likely, Slide, Unlikely)	(30, 70)
(Very Likely, Slide, Likely)	(10, 90)
(Very Likely, Rock, Unlikely)	(10, 90)
(Very Likely, Rock, Likely)	(1, 99)

Table 3.16 Description of CPT for node variable "transformer damage"

(Foundation failure, Failure of component class 1, Failure of component class 1)	Tranformer damage (Low, Medium, High)
(Unlikely, Unlikely, Unlikely)	(99, 1, 0)
(Unlikely, Unlikely, Likely)	(20, 60, 20)
(Unlikely, Likely, Unlikely)	(5, 30, 65)
(Unlikely, Likely, Likely)	(3, 20, 77)
(Likely, Unlikely, Unlikely)	(5, 25, 70)
(Likely, Unlikely, Likely)	(2, 15, 83)
(Likely, Likely, Unlikely)	(0, 10, 90)
(Likely, Likely, Likely)	(0, 1, 99)

The assumption behind generating Table 3.13 was that foundation failure is more likely when transformer rocking and liquefaction occurrence probability are high. Table 3.14 shows that when the transformer is in rocking mode and there is a high chance of liquefaction occurrence, the failure of component class 1 is likely. When it is in rest mode and there is no probability of liquefaction occurrence, failure probability is very low, and when it is in slide mode it is considered to have low probability of failure. Table 3.15 was generated based on the assumption that there will be a higher probability of failure of the component class 2 when conductor failure, foundation failure, and transformer rocking occur, and vice versa. Finally, Table 3.16 was generated based on the assumption that failure of foundation and component class 1 cause more damage to the transformer, hence the damage probability is higher. The failure of component class 2 will not cause severe damage to the transformer, as it is possible to replace such components more easily. In fact, some substations keep spare porcelain bushings, lightning arresters and tertiary bushings.

3.6 Sensitivity analysis

Since BBN employs prior conditional probabilities; it is essential to carry out the sensitivity analysis to understand the significance of input parameters to the output results. In literature, different methods have been proposed to perform sensitivity analysis in a BBN (Jensen 1996; Pearl 1988). The variance reduction method was used in this thesis to determine the sensitivity of output parameter regarding the variation of a particular input parameter. This method was chosen as the input parameters needed to assess the transformer damage had discrete and continuous values (Norsys Software Corp 2006; Pearl 1988) and was applied for similar application (Cockburn and Tesfamariam 2012; Ismail et al. 2011; Tesfamariam and Martín-Pérez 2009). The method implies computation of variance

reduction of the expected real value of a query node Q (e.g., transformer damage) due to varying variance node F (e.g., PGA, liquefaction). Therefore, the variance of the real value of Q given evidence F, $V(q|f)$, is computed as (Norsys Software Corp 2006; Pearl 1988),

$$V(q \mid f) = \sum_{q} p(q \mid f)[X_q - E(Q \mid f)]^2 \quad \textbf{3.4}$$

where q is the state of the query node Q, f is the state of the varying variable node F, $p(q|f)$ is the conditional probability of q given f, X_q is the numeric value corresponding to state q, and $E(Q|f)$ is the expected real value of Q after the new finding f for node F.

Results of the sensitivity analysis for the model illustrated in Figure 3.2 are summarized in Table 3.17. Table 3.17 shows the variance reduction and normalized percent contribution of the main input variables. The percent contribution values are normalized with respect to the sum of all the percent contribution of the input parameters. d, M_w, and S_T showed the highest normalized percent contribution towards the variance reduction, 67%, 16.12%, and 15.12%, respectively. To a lesser degree, the rest of the input variables showed normalized percent contribution less than 1%. Results of this analysis showed that the seismic hazard has the most contribution to the results and the sensitivity of the parent node (i.e., d, M_w, S_T, ECL) significantly depends on the variability of the dependent children (i.e., PGA, conductor failure, liquefaction, RCL). This indeed highlights the need for rigorous method of quantifying site seismicity (e.g. see Bensi et al. 2011) and incorporation of mitigation techniques to delineate the seismic demand (e.g. use of base isolation).

Table 3.17 Sensitivity analysis for "transformer damage" using proposed BBN model

Node	Variance reduction	Normalized percent contribution
D	3.62E-02	67.00%
M_w	8.73E-03	16.12%
S_T	8.19E-03	15.12%
ECL	4.11E-04	0.76%
σ_{vo}	2.41E-04	0.44%
q_c	1.32E-04	0.24%
Anchorage	1.18E-04	0.22%
B/H	6.01E-05	0.11%
D_{50}	3.67E-06	0.007%

Chapter 4: Predictive Model Development

This chapter consists of two main sections, development of predictive model using Markov chain, and response surface method (RSM). By creating different scenarios in the BBN framework (as shown in Chapter 3), these analyses were performed.

4.1 Model development using Markov chain

To understand the pattern of change of low, medium and high transformer damage probabilities with the change of PGA, 10,000 random values of the input parameters (PGA, B/H, σ_{vo}, q_c, D_{50}, ECL) were generated. The simulations were done for anchored and unanchored transformer separately. The results were plotted and fitted for low, medium and high transformer damage probability (see Figure 4.1 and Figure 4.2). The pattern of the graphs for states, low, medium and high, show that the probabilities decrease gradually for low damage state, on the other hand, the probabilities increase gradually for high damage state. The probabilities for medium damage states increase for a certain time and after reaching a peak the probabilities decrease. The trend of the probabilities for low, medium and high damage states in the graphs follows the Markov property. A stochastic process has the Markov property if the conditional probability distribution of the future state only depends on the present state (Feller 1971).

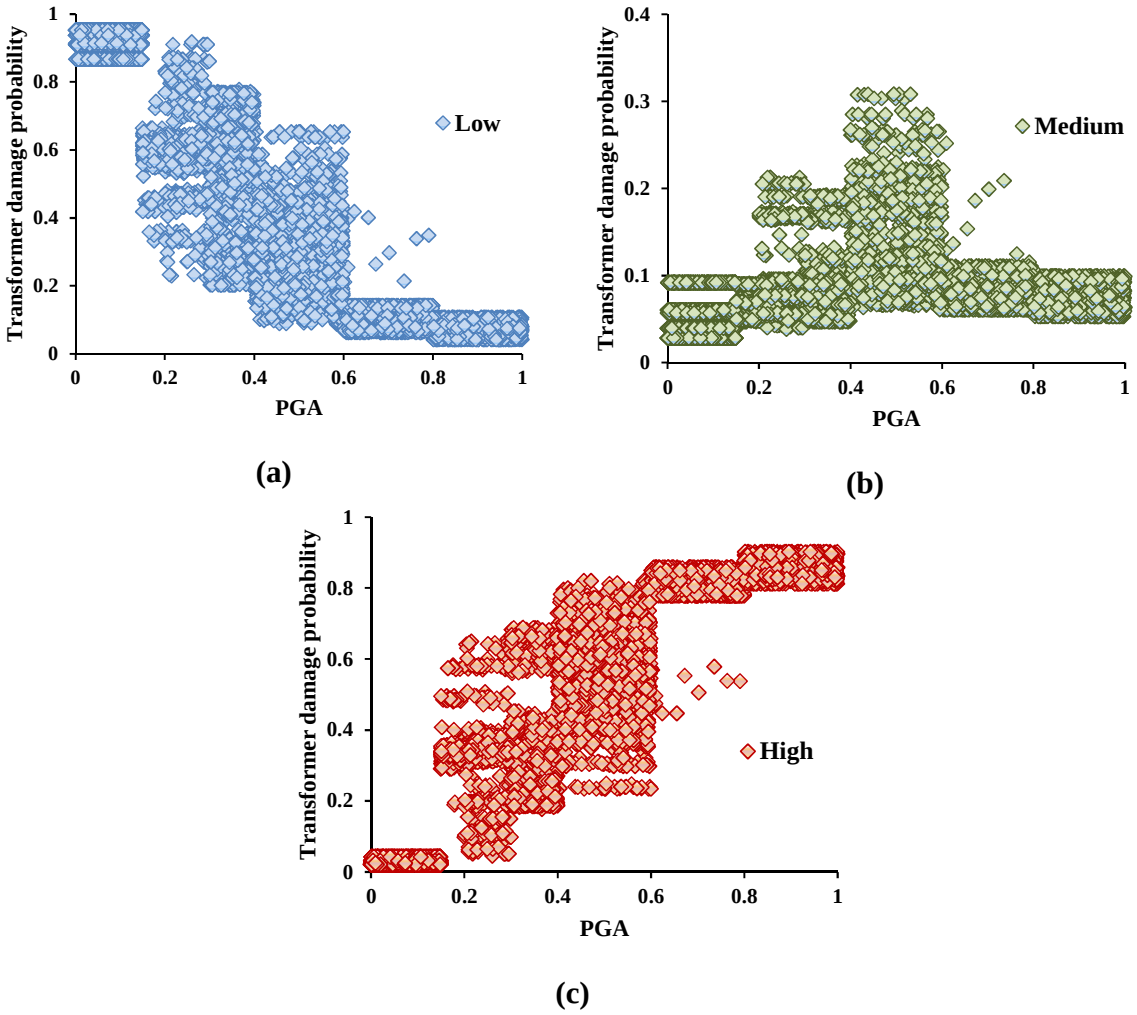

Figure 4.1 Simulated data plotted for (a) Low, (b) Medium and (c) High damage states of anchored transformer

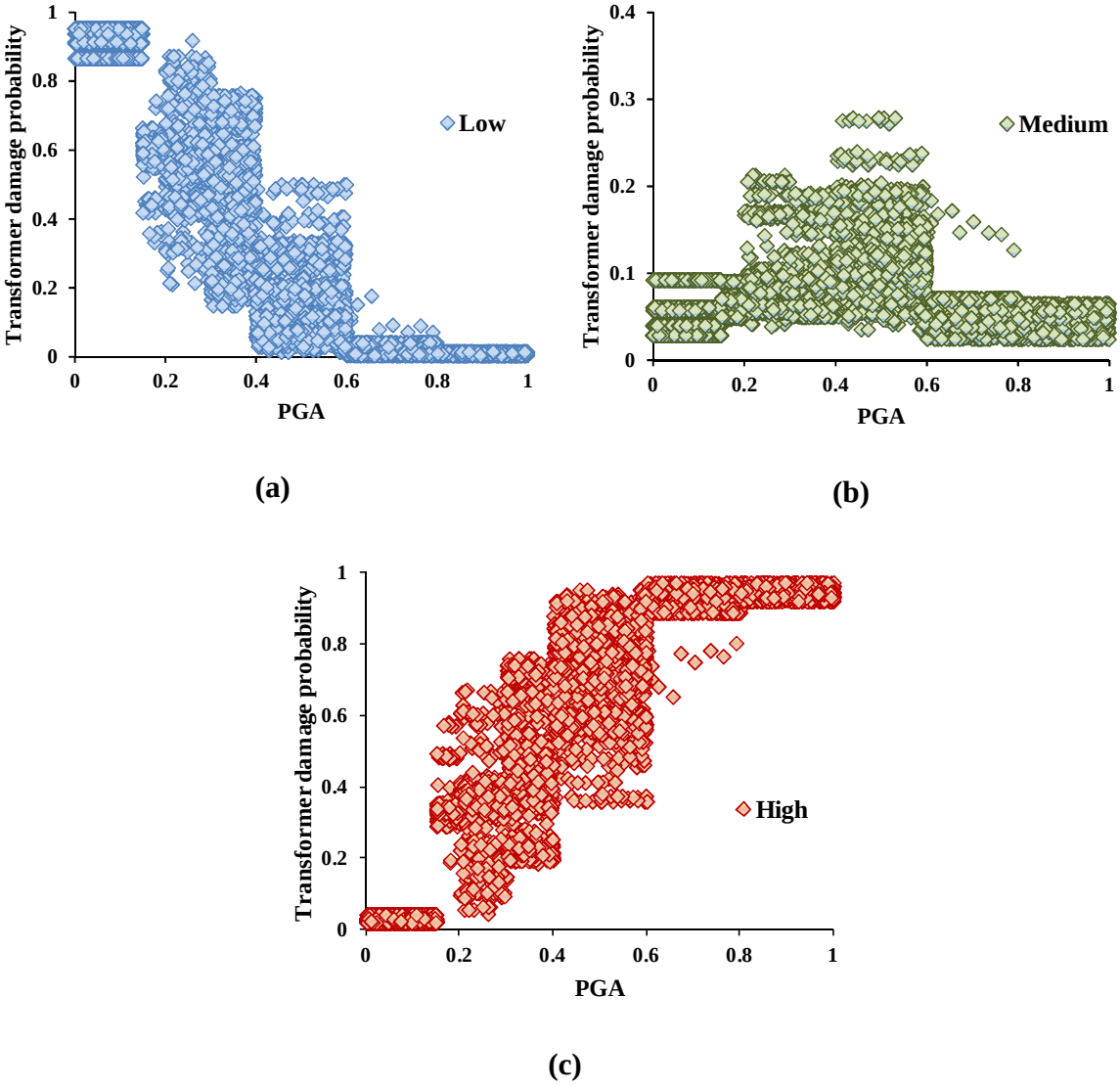

Figure 4.2 Simulated data plotted for (a) Low, (b) Medium and (c) High damage states of unanchored transformer

The Markov chain model was developed using the simulation data. This model is widely known in developing a deterioration model of civil infrastructure (Baik et al. 2006; Enright and Frangopol 1999; Morcous and Lounis 2007). The Markov chain is a stochastic process whose development can be treated as a series of transitions between certain states (Lounis et al. 1998; Morcous 2006). The process will be considered as a first order Markov

process if the probability of being in a future state only depends on a present state and not on how it is achieved (Parzen 1962). This property can be given as follows, for a discrete parameter stochastic process (X_i) with a discrete state space,

$$P(X_{i+1} = i_{i+1} | X_t = i_t, X_{t-1} = i_{t-1}, \dots, X_1 = i_1, X_0 = i_0) = P(X_{t+1} = i_{i+1} | X_t = i_t) \quad \textbf{4.1}$$

where i_t= state of the process at time t; and P= conditional probability of any future event given the present and past event. In this thesis, Markov chain was used to predict the transformer damage probability for different discrete damage states (i.e., low, medium, and high) and accumulating the probability of transition from one state to another over multiple discrete PGA interval. Transition probabilities are usually represented by a matrix of order ($n \times n$) and called the transition probability matrix is represented by P. Here, n is the number of condition states (e.g., for this thesis, $n = 3$). The transition probability matrix can be represented as follows,

$$P = \begin{bmatrix} p_{1,1} & p_{1,2} & \cdots & p_{1,n} \\ p_{2,1} & p_{2,2} & \cdots & p_{2,n} \\ . & . & \cdots & . \\ . & . & \cdots & . \\ . & . & \cdots & . \\ p_{n,1} & p_{n,2} & \cdots & p_{n,n} \end{bmatrix} \quad \textbf{4.2}$$

where each element, $p_{i,j}$ in the matrix represents the probability that a condition of the transformer damage will go from state i to state j during a certain PGA interval. If the initial condition vector $P(0)$ of the transformer is known, the future condition vector $P(t)$ at any number of PGA intervals (t) can be presented as follows (Morcous 2006),

$$P(t) = P(0) \times P^t \quad \textbf{4.3}$$

The transition probability matrix of transformer damage for anchored and unanchored condition was developed using the simulated data. It was calculated based on the condition that it minimizes the root mean square estimation of distance between the Markovian expected value of the state and the damage probabilities for that state as predicted by the BBN framework. The transition probability matrix for anchored and unanchored transformer for estimating transformer damage probabilities are given in Equation 4.4 and 4.5.

$$P_{Anchored} = \begin{bmatrix} 0.989 & 0.011 & 0.000 \\ 0.000 & 0.956 & 0.044 \\ 0.000 & 0.000 & 1.000 \end{bmatrix} \quad \textbf{4.4}$$

$$P_{Unanchored} = \begin{bmatrix} 0.980 & 0.020 & 0.000 \\ 0.000 & 0.920 & 0.080 \\ 0.000 & 0.000 & 1.000 \end{bmatrix} \quad \textbf{4.5}$$

The transition probability graphs with the change of PGA values are also given in Figure 4.3 and Figure 4.4. The graphs show that the low state transition probabilities for unanchored transformer decreases more quickly than the anchored transformer and the high state transition probabilities reach more quickly to 100% for unanchored transformer in comparison to anchored transformer. That means the Markov model shows that with the use of anchorage, as expected, the transformer damage probability is reduced.

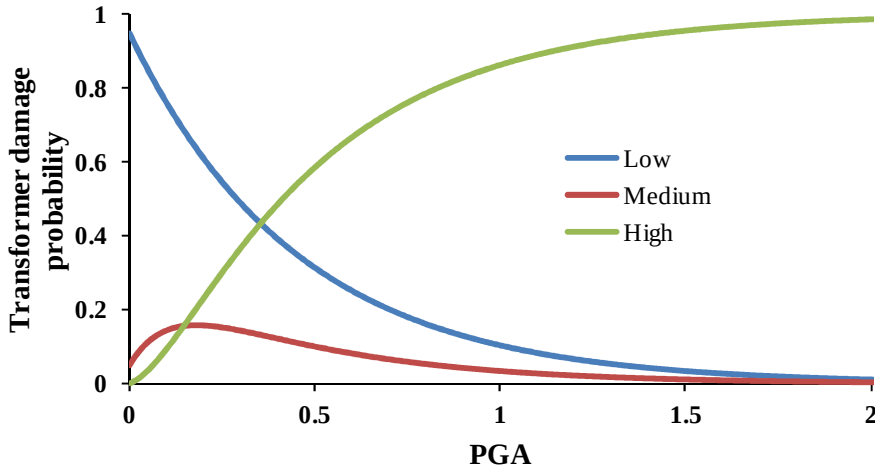

Figure 4.3 Transition probabilities calculated using Markov chain for anchored transformer

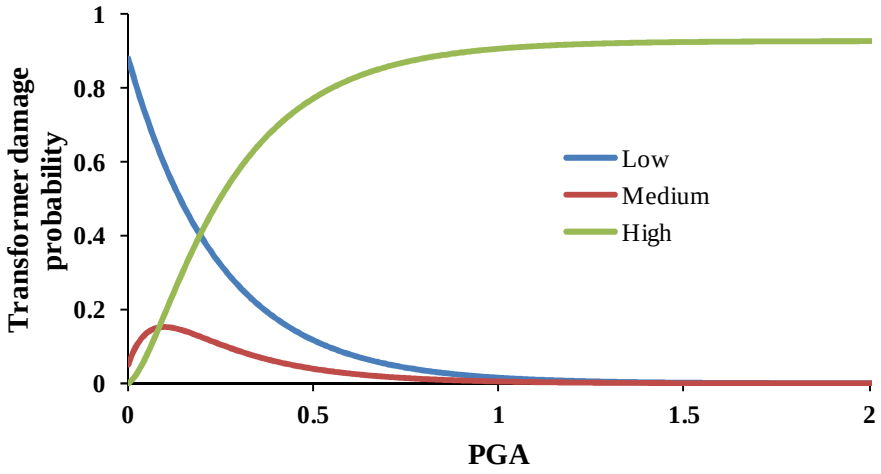

Figure 4.4 Transition probabilities calculated using Markov chain for unanchored transformer

4.2 Predictive model development using RSM

This thesis aims at the screening of important variables followed by developing an adequate functional relationship between the response of interest (i.e., transformer damage probability) and the associated input variables (i.e., M_w, d, S_T, ECL, B/H, etc.) using a response surface method (RSM) approach. Several researchers have used RSM in different engineering application(Buratti et al. 2010; Möller et al. 2009; Rajeev and Tesfamariam

2012; Zhou et al. 2013). If the response of interest is denoted by y, and the associated input variables are denoted as $x_1, x_2, x_3, \ldots . x_K$, the unknown relationship between them can be approximated by response surface methodology which consists of a group of mathematical and statistical techniques (Khuri and Mukhopadhyay 2010). Two main approximations are commonly used in RSM, first order model or polynomial of higher degree (such as second degree model)(Rajeev and Tesfamariam 2012). The relationship can be represented by a low degree polynomial model of the form,

$$y = f'(x)\beta + \epsilon \quad \textbf{4.6}$$

where, $x = (x_1,\ x_2, x_3 \ldots \ldots \ldots, x_k)'$, $f(x)$ is a vector function of p elements that consists of powers and cross products of powers of $x_1, x_2, x_3, \ldots \ldots, x_k$ up to a certain degree denoted by $d(\geq 1)$, β is a vector of p unknown constant coefficient referred to as parameters and ϵ is a random experimental error assumed to have a zero mean.

Design Expert V8 (2009) software was used to perform the screening and RSM approach. A fractional factorial design (Resolution IV design) consisting of 18 runs was used to screen the most important input variables (i.e., M_W, d, S_T, ECL, B/H, σ_{vo}, q_c, and D_{50}) for anchored and unanchored transformer. The response of the input variables is denoted as transformer damage probability. For the study of the prediction model, mean transformer damage probability was used (instead of using different states).

Resolution IV designs were used because they are useful for screening of main effects and it allows to determine if interactions exists (User manual of Design Expert V8 (2009)). The analysis results provide half normal plot and Pareto chart to screen the important variables. After selecting the important variables based on t-values and Bonferroni limits,

analysis of variance (ANOVA) along with its significance level was generated. After that the model significance was tested and the model was further used to select the important variables. The most significant factors or variables were studied later on using RSM approach. Design Expert V8 (2009) has an option named 'optimal RSM approach' which is useful to create a good design for fitting a linear, quadratic, cubic model and higher (up to 6^{th}) order models. Optimal RSM approach was further used to generate an approximate relationship between the response and significant variables.

4.2.1 Screening of input variables

Instead of 256 experimental runs as per full factorial design (2^8), just 18 runs were performed as per Resolution IV design. It reduced the run without much compromise on errors. Each of the parameters varied with two levels, i.e., M_W (5.5 and 7.5), d (0 and 80 km), S_T (150 and 1890 m/sec), σ_{vo} (0 and 300 KPa), q_c (0 and 30 MPa), D_{50} (0 and 0.6 mm) and ECL (1 and 1000 mm). The Pareto chart gave that the M_W, d, S_T, B/H, σ_{vo}, q_c, and ECL are the most significant factors for both anchored and unanchored transformer (Figure 4.5 and Figure 4.7). Thus, these variables were taken as model variables and the ANOVA model was constructed. Both of the models were found significant (for anchored $p<0.0001$ and unanchored $p=0.0002$) and the models passed the normal distribution test too (Figure 4.6 and Figure 4.8).

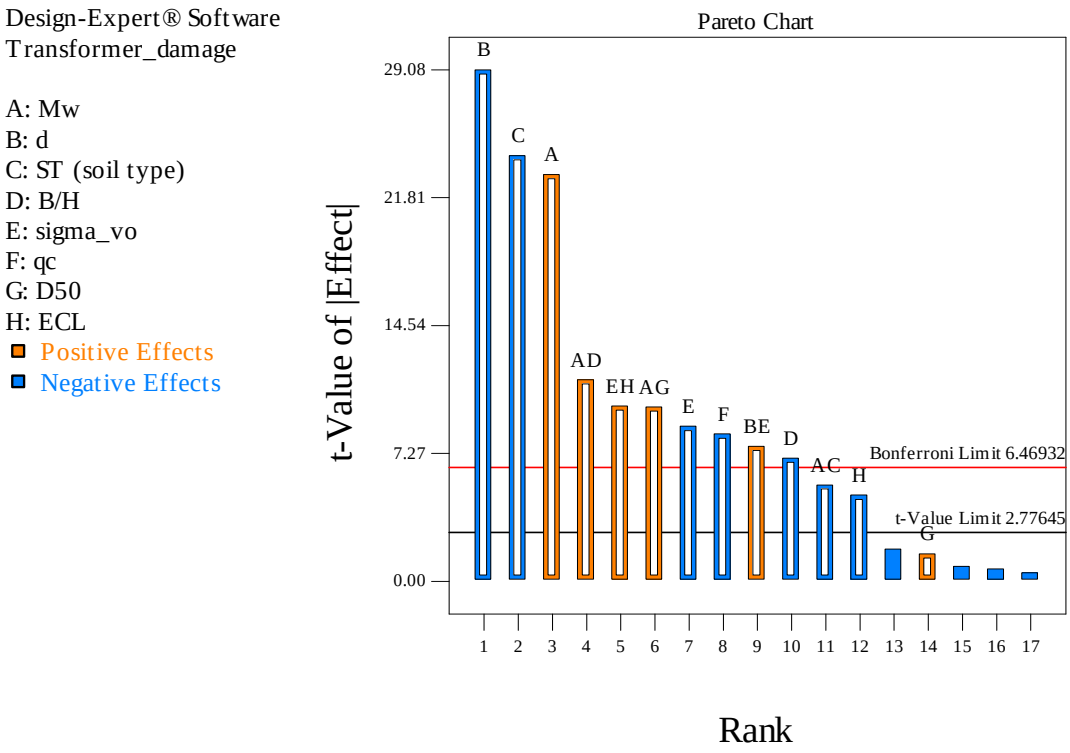

Figure 4.5 Screening of important variables for transformer (Anchored) damage probability calculation using a Pareto chart

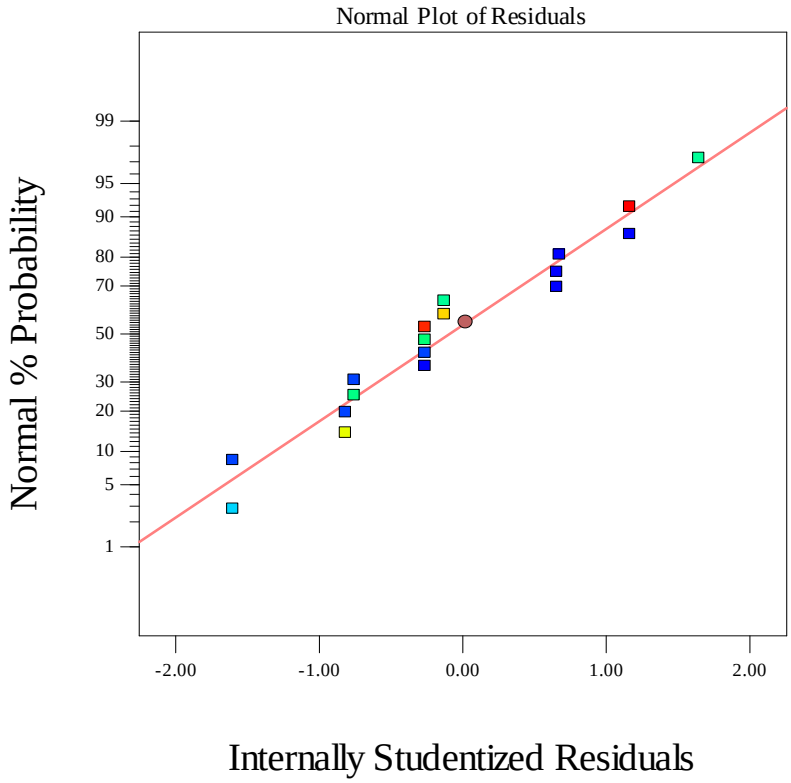

Figure 4.6 The internally studentized residuals and normal % probability plot of tranformer (Anchored) damage probability for the Resolution IV design

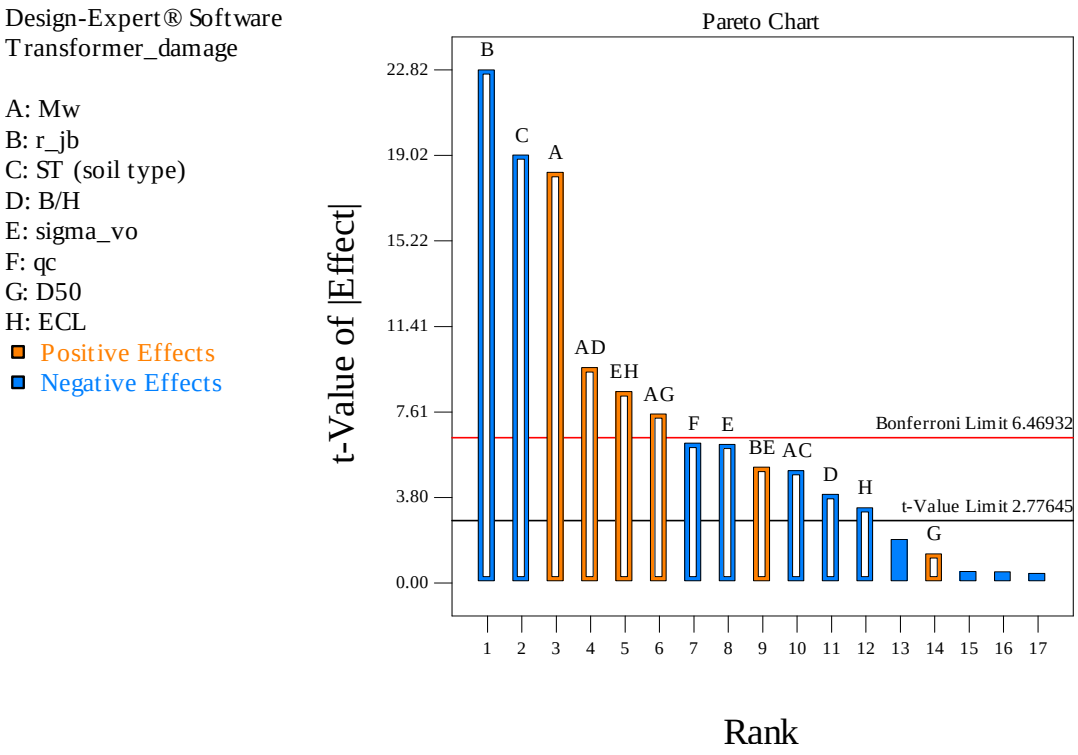

Figure 4.7 Screening of important variables for transformer (Unanchored) damage probability calculation using a Pareto chart

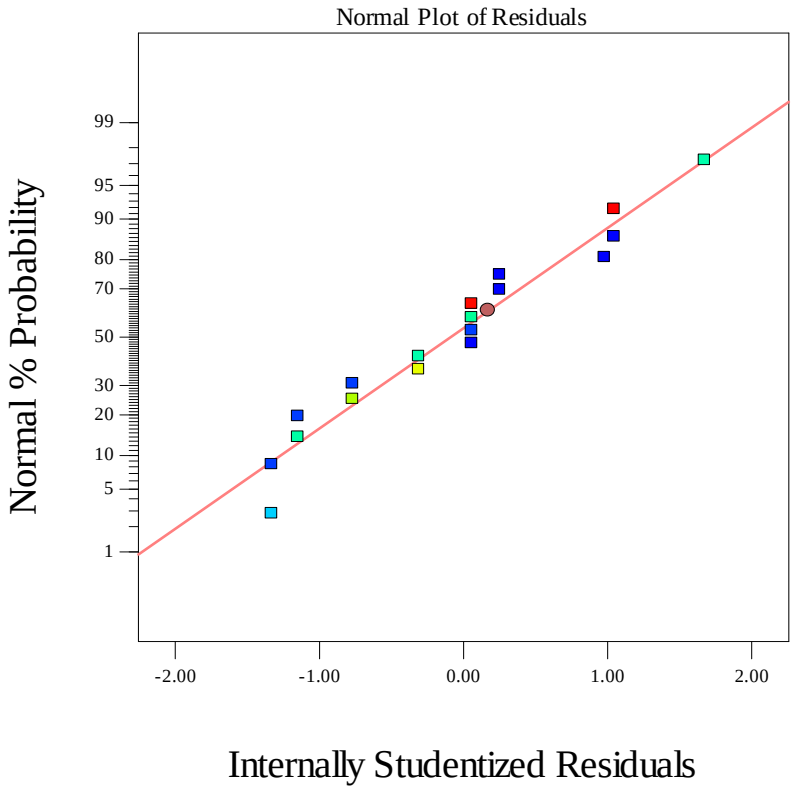

Figure 4.8 The internally studentized residuals and normal % probability plot of tranformer (Unanchored) damage probability for the Resolution IV design

4.2.2 Prediction equation using Response Surface Method (RSM)

The significant variables found in screening (M_W, d, S_T, B/H, σ_{vo}, q_c, and ECL) were selected for further analysis using RSM approach. A total of 315 runs were conducted using optimal RSM analysis for both anchored and unanchored transformer. In this thesis, three of the variables were discrete (M_W, S_T, and B/H) and rest of them were continuous (d, σ_{vo}, q_c, and ECL). Five discrete values of M_w = {5.5, 6, 6.5, 7, 7.5} and S_T = {150 m/sec, 250 m/sec, 520 m/sec, 1070 m/sec, 1890 m/sec}, and three discrete values of B/H = {0.34, 0.5, 0.69} were varied in the model. On the other hand, two levels (low to high) were varied for continuous variables in the model, i.e., d = [0, 80 km], σ_{vo} = [0, 300 kPa], q_c = [0, 30 MPa] and ECL = [1, 1000 mm].

For anchored transformer, the model summary showed quadratic as the most significant model (p<0.0001) with non-significant lack of fit. Analysis of ANOVA showed that M_w, d, S_T, σ_{vo}, ECL, $M_w \times d$, $M_w \times S_T$, $d \times S_T$, $d \times \sigma_{vo}$, d^2, ${S_T}^2$, and ${q_c}^2$ were the most significant. Rest of the main variables and their interactions had p-values greater than 5% significance level. Thus, the model was again generated with the significant variables and their interactions. As q_c did not have any significance, the higher level interaction of q_c (i.e., ${q_c}^2$) was ignored in further analysis. The reduced quadratic model was again found significant with p-value <0.001. The normal plot of residuals (Figure 4.9) and the actual vs. predicted plot (Figure 4.10) satisfied the normal distribution and prediction capability.

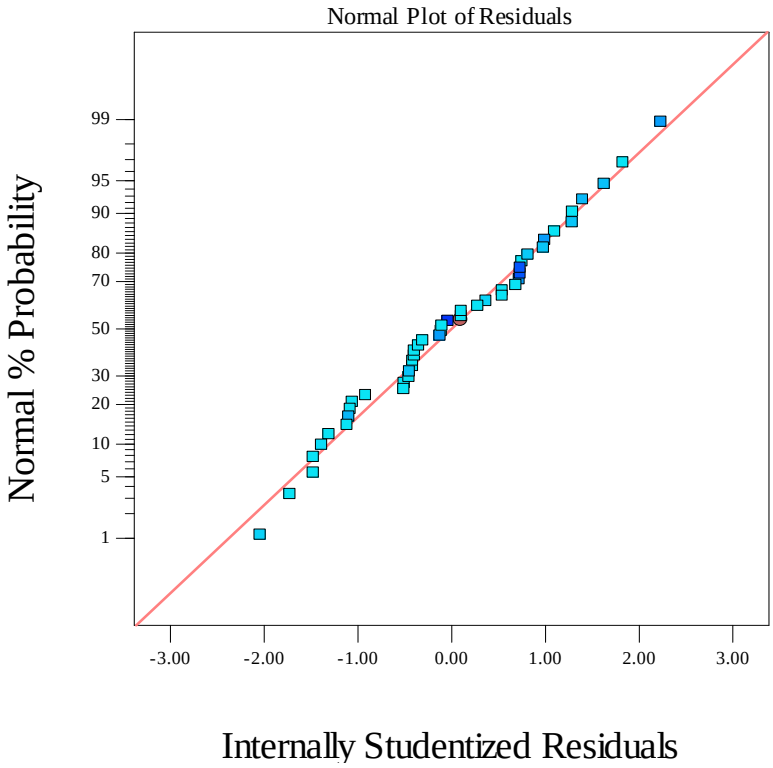

Figure 4.9 The internally studentized residuals and normal % probability plot of tranformer (Anchored) damage probability for quadratic model

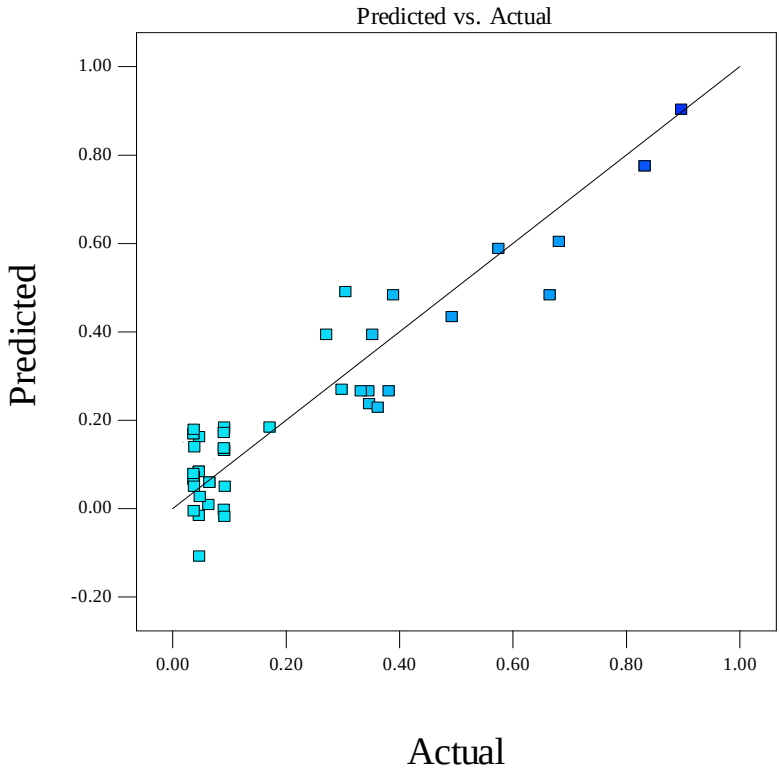

Figure 4.10 The actual and predicted plot of tranformer (Anchored) damage probability using quadratic model

For unanchored transformer, the model summary also showed quadratic as the most significant model with non-significant lack of fit. Analysis of ANOVA showed that M_w, d, S_T, σ_{vo}, ECL, $M_w \times d$, $M_w \times S_T$, $d \times S_T$, $d \times \sigma_{vo}$, $S_T \times B/H$, d^2, ${S_T}^2$, ${q_c}^2$ and ECL^2 were the most significant. The rest of the main variables and their interactions had p-values greater than 5% significance level. Thus, the model was again generated with the significant variables and their interactions. As B/H and q_c did not have any significance, the higher level interactions of B/H and q_c (i.e., $S_T \times B/H$ and ${q_c}^2$) were ignored in further analysis. The reduced quadratic model was again found significant with p-value <0.001. The normal plot of residuals (Figure 4.11) and the actual vs. predicted plot (Figure 4.12) satisfied the normal distribution and prediction capability.

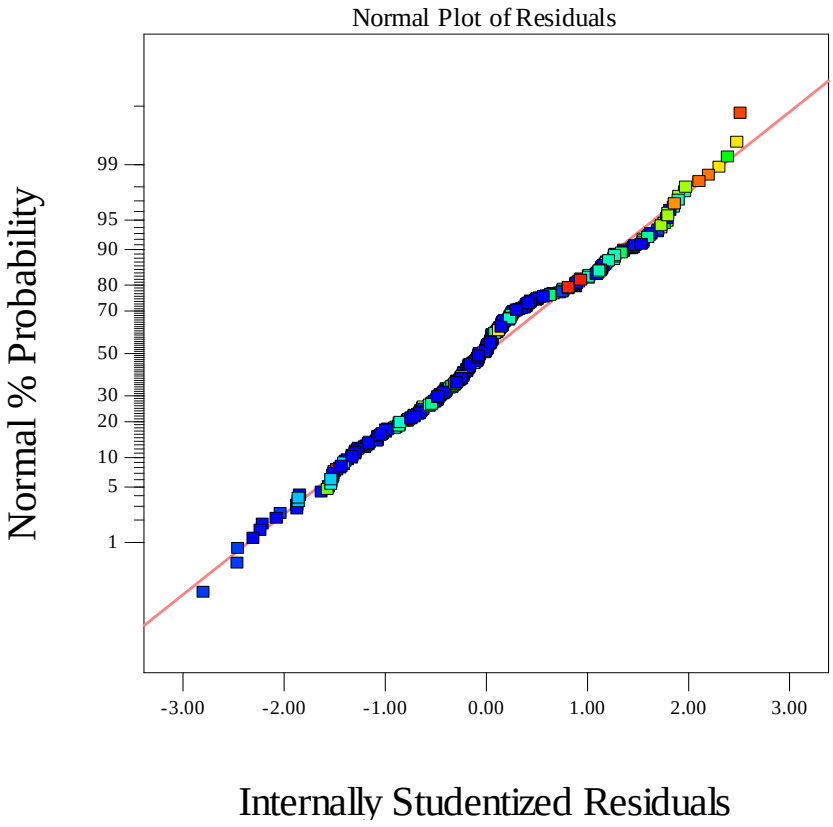

Figure 4.11 The internally studentized residuals and normal % probability plot of tranformer (Unanchored) damage probability for quadratic model

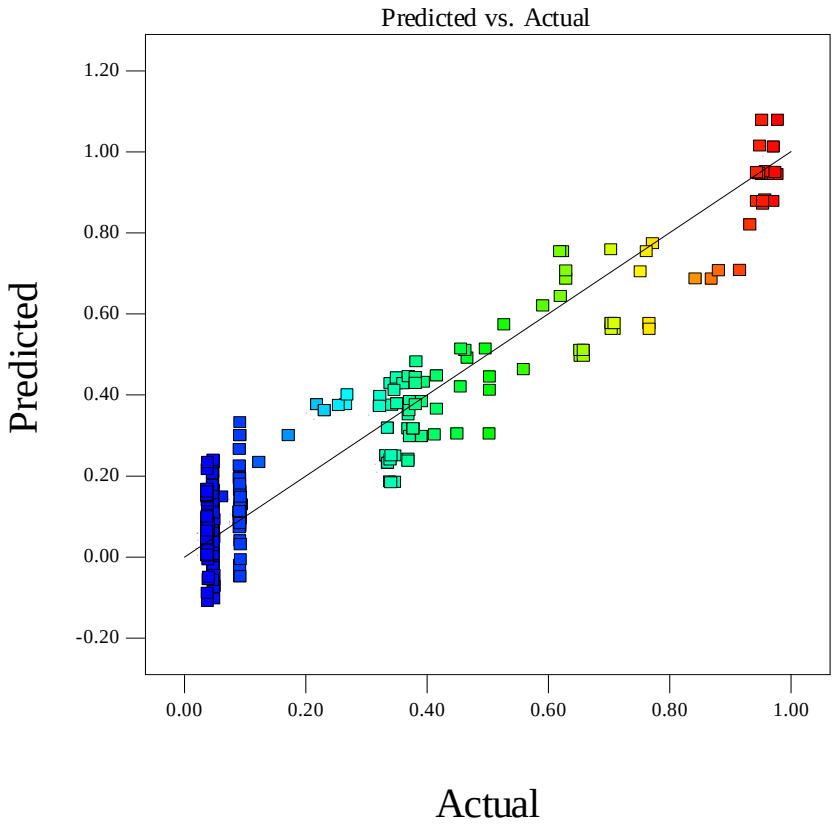

Figure 4.12 The actual and predicted plot of tranformer (Unanchored) damage probability using quadratic model

The final predictive equations are given in Equations 4.7 and 4.8 for anchored and unanchored transformers, respectively.

$$\begin{aligned} Transformer\ damage\ probability \\ &= -0.79436 + 0.24306 \times M_w - 6.08641E^{-03} \times d \\ &+ 1.21407E^{-04} \times S_T - 4.24104E^{-04} \times \sigma_{vo} - 7.2997E^{-05} \times ECL \\ &- 1.6282E^{-03} \times M_w \times d - 6.6912E^{-05} \times M_w \times S_T + 1.71676E^{-06} \\ &\times d \times S_T + 6.01768E^{-06} \times d \times \sigma_{vo} + 1.19735E^{-04} \times d^2 \\ &+ 6.11752E^{-08} \times {S_T}^2 \end{aligned} \quad \textbf{4.7}$$

$$\begin{aligned} Transformer\ damage\ probability \\ &= -0.87825 + 0.26834 \times M_w - 5.77915E^{-03} \times d \\ &+ 1.21610E^{-04} \times S_T - 4.46855E^{-04} \times \sigma_{vo} - 1.95185E^{-04} \times ECL \\ &- 1.94687E^{-03} \times M_w \times d - 6.8807E^{-05} \times M_w \times S_T + 2.14197E^{-06} \\ &\times d \times S_T + 6.35941E^{-06} \times d \times \sigma_{vo} + 1.2883E^{-04} \times d^2 \\ &+ 5.20427E^{-08} \times {S_T}^2 + 1.28913E^{-07} \times ECL^2 \end{aligned} \quad \textbf{4.8}$$

Figure 4.13 and Figure 4.14 show the interactions between the variables d and S_T has a positive effect on the response, for both anchored and unanchored transformer.

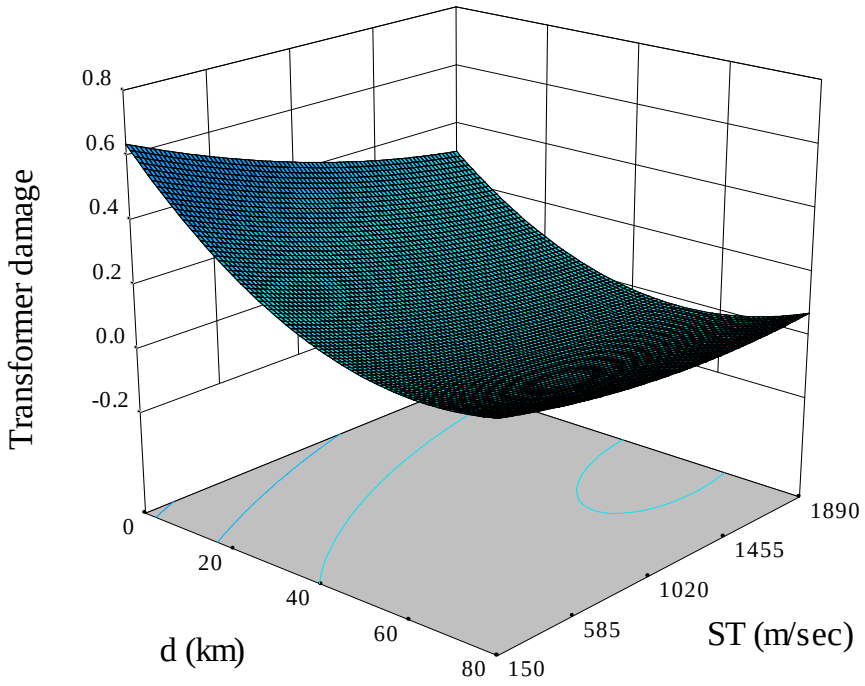

Figure 4.13 3-D interaction plot for d (fault to site distance in km) and S_T (soil type, defined by shear wave velocity of soil, in m/sec) in the quadratic model (for anchored transformer)

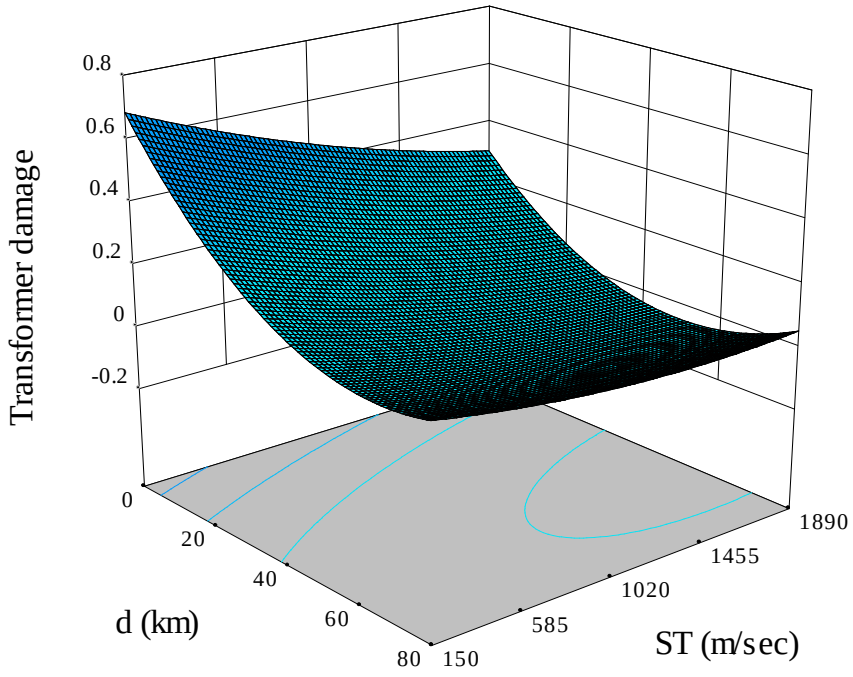

Figure 4.14 3-D interaction plot for d (fault to site distance in km) and S_T (soil type, defined by shear wave velocity of soil, in m/sec) in the quadratic model (for unanchored transformer)

4.2.3 Model validation

To validate the predictive equations, again 10,000 random runs were generated by randomly changing the eight input variables (i.e., M_W, d, S_T, B/H, σ_{vo}, q_c, D_{50}, and ECL) for both anchored an unanchored transformer. The input values of the variables are shown in Figure 4.15 in bar charts. The results from the BBN framework were compared with the results found using the prediction equation. Figure 4.16 and Figure 4.17 show comparison between the actual and predicted values of transformer damage probability for anchored and unanchored conditions, respectively. The graphs show how the data points are scattered over the line of equality. For the anchored transformer the model predicted comparatively well in compared to unanchored transformer. Both of the graphs show that models predict well for the high values of transformer damage probability. On the other hand, while predicting the

low transformer damage probability the model predicted values less than zero in some cases. This is the weakness of the predictive model.

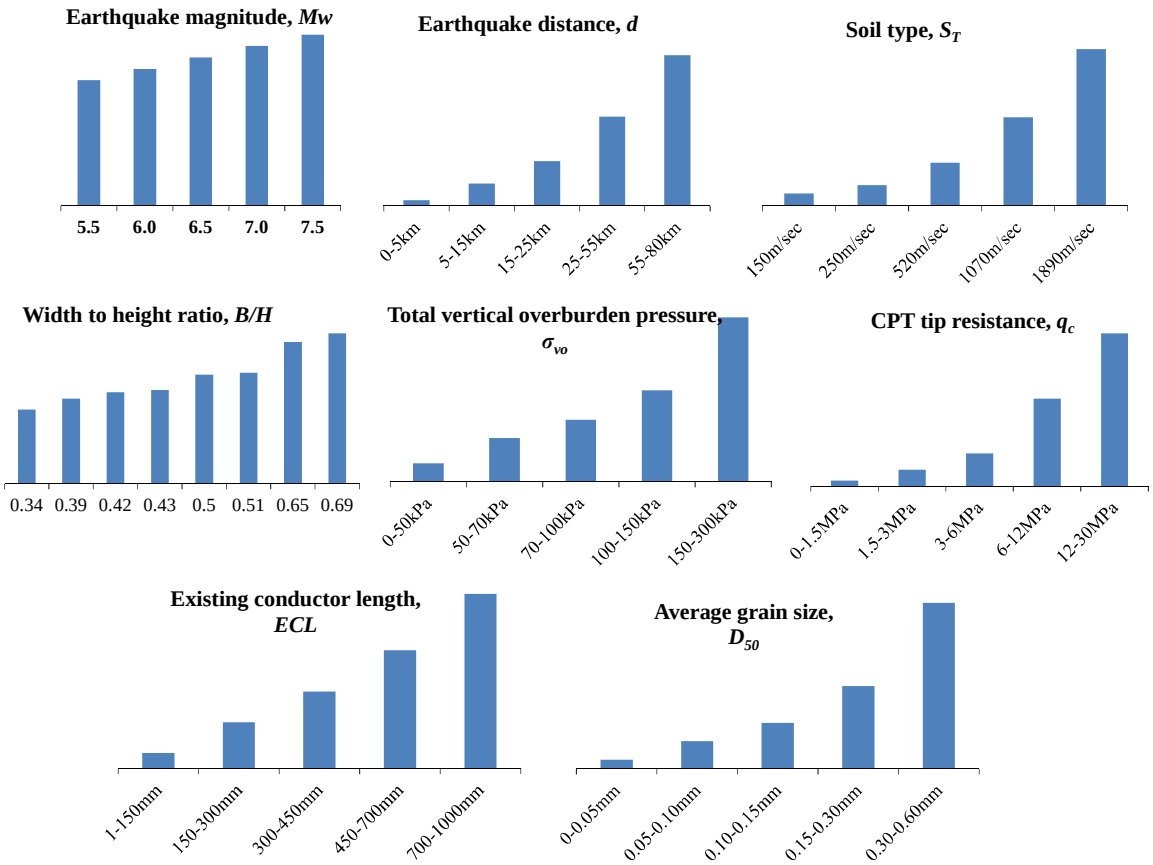

Figure 4.15 Bar charts showing the range of values of input variables

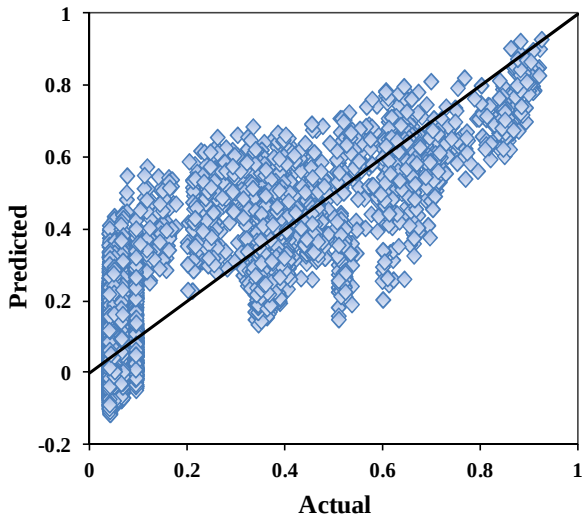

Figure 4.16 Model validation for anchored transformer

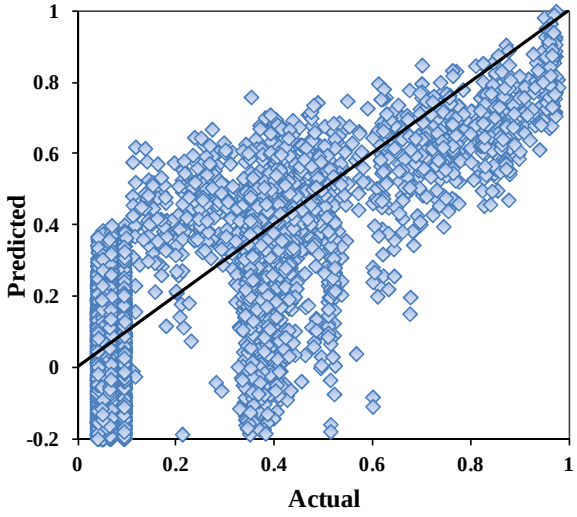

Figure 4.17 Model validation for unanchored transformer

Chapter 5: Conclusion and Future Work

Based on the observed failure from the past earthquakes, this thesis proposed a risk assessment framework using BBN, for high-voltage transformers. Cause and effect analysis of the transformer vulnerability showed that the transformer damage is initiated due to soil instability, rocking response and interaction coming from conductors, due to the relative movement of the substation components. This thesis used information from published literature to develop the conditional probability tables in BBN. The framework predicts the damage probability of a high-voltage transformer subjected to seismic events.

Using the proposed framework a sensitivity analysis was performed. The sensitivity analysis showed that the input parameters related to seismic hazard had more contribution towards the transformer damage and average grain size (D_{50}) has lowest contribution towards the transformer damage. Hence, the best strategy is to reduce the PGA at the transformer base that could be confirmed by using the base isolation at the transformer base.

After that, response surface method (RSM) was used to develop a predictive model. To perform the RMS an initial screening was performed as the number of input variables are more than five. The results from screening showed that average grain size (D_{50}) had insignificant contribution to the transformer damage probability, similar to the sensitivity analysis. Two quadratic equations were developed using RSM for anchored and unanchored transformers, to predict the mean probability of transformer damage. Finally, for different combinations of input variables, the transformer damage probability was calculated using the predictive model and compared with the actual one. Both of the results for anchored and unanchored transformer showed that models predict well for the high values of transformer

damage probability. On the other hand, for the low transformer damage probability, the model predicted values less than zero in some cases. This is the weakness of that predictive model.

Another analysis was performed by doing 10,000 simulations with randomly generated eight input variables. The output data (transformer damage probabilities in different states, i.e., low, medium, and high) was then plotted to understand the pattern of the dataset. The result showed that the damage probabilities of different states followed the Markov property. Therefore, in the end of the case study, the transition probability matrices for anchored and unanchored transformer were developed, to predict the probability of transformer damage in different states (i.e., low, medium, high) with the change of PGA values.

The results are particularly useful supporting decisions on mitigation measures and seismic risk prediction in a region. One of the major advantages with BBN frameworks is that when new information is available it can be updated very easily. This intuitive nature is also useful for different stakeholders. Note that BBNs could also benefit from analytical and experimental results, which are typically explored for single failure modes of substation components, but that can be systematically integrated through BBNs. This thesis combined most of the critical failure modes observed for high-voltage transformers to date.

The main limitation of the current study is that several conditional probabilities in the transformer vulnerability assessment were knowledge based. This may change with the perspective of researchers and the stakeholders. However the methodology is ready to accept conditional probabilities that are developed based on other evidence data (i.e., historical data,

results from analytical and experimental work). For future study this part could be refined. Also, this thesis showed risk assessment of high voltage transformer without considering any retrofitting options. Further study can be carried out by including retrofitting options to the transformer components. This thesis can also be expanded by including other causes of failure of high voltage transformer (e.g., deterioration due to ageing, failure due to multi-hazard).

References

Abdelgawad, M., and Fayek, A. R. (2012). "Comprehensive hybrid framework for risk analysis in the construction industry using combined failure mode and effect analysis, fault trees, event trees, and fuzzy logic." *Journal of Construction Engineering and Management*, 138(5), 642–651.

Abdelmoumene, A., and Bentarzi, H. (2012). "Reliability enhancement of power transformer protection system." *Journal of Basic and Applied Scientific Research*, 2(10), 10534–10539.

Abogrean, E. M., and Latif, M. (2012). "Application of the Bayesian network to machine breakdowns using witness simulation." *The World Congress on Engineering*, Vol. I, London, UK.

Abrahamson, N. A., and Silva, W. J. (1997). "Empirical response spectral attenuation relations for shallow crustal earthquakes." *Seismological Research Letters*, 68(1), 94–127.

Anagnos, T. (1999). *Development of an electrical substation equipment performance database for evaluation of equipment fragilities*. PEER 2001/06, Pacific Earthquake Engineering Research Center, University of California, Berkeley, USA.

ASCE. (1999). *Guide to improved earthquake performance of electric power systems*. (A. J. Schiff and ASCE, eds.), 1801 Alexander Bell Drive Reston, Virginia 20191-4400, ASCE Manuals and Reports on Engineering Practice No. 96, 65–226.

Ashrafi, A. (2003). "Issues of seismic response and retrofit for critical substation equipment." M.Sc. dissertation, New Jersey Institute of Technology, Newark, NJ, USA.

Atkinson, G. M., and Boore, D. M. (1995). "New ground motion relations for eastern North America." *Bulletin of the Seismological Society of America*, 85(1), 17–30.

Atkinson, G. M., and Boore, D. M. (1997). "Stochastic point-source modeling of ground motions in the Cascadia region." *Seismological Research Letters*, 68(1), 74–85.

Aven, T. (2008). *Risk analysis: assessing uncertainities beyond expected values and probabilities*. John Wiley & Sons,Ltd, West Sussex, England.

Baik, H. S., Jeong, H. S., and Abraham, D. M. (2006). "Estimating transition probabilities in Markov chain-based deterioration models for management of wastewater systems." *Journal of Water Resources Planning and Management*, 132(1), 15–24.

Baker, J. W. (2008). *An introduction to probabilistic seismic hazard analysis (PSHA)*. Version 1.3, Report for the US Nuclear Regulatory Commission.

Balakrishnan, M., and Trivedi, K. S. (1996). “Stochastic Petri nets for the reliability analysis of communication network applications with alternate-routing.” *Reliability Engineering & System Safety*, 52(3), 243–259.

Bayraktarli, Y. Y. (2006). “Application of Bayesian probabilistic networks for liquefaction of soil.” *6th International PhD Symposium in Civil Engineering*, Zurich, Switzerland, 1–8.

Bayraktarli, Y. Y., Ulfkjaer, J., Yazgan, U., and Faber, M. (2005). “On the application of Bayesian probabilistic networks for earthquake risk management.” *The 9th International Conference on Structural Safety and Reliability*, Rome, Italy, 3505–3512.

Bayraktarli, Y. Y., Yazgan, U., Dazio, A., and Faber, M. (2006). “Capabilities of the Bayesian probabilistic networks approach for earthquake risk management.” *First European Conference on Earthquake Engineering and Seismology*, Geneva, Switzerland, 1–10.

Bensi, M. T., Der Kiureghian, A., and Straub, D. (2009). “A Bayesian network framework for post-earthquake infrastructure system performance assessment.” *TCLEE 2009: Lifeline Earthquake Engineering in a Multihazard Environment ©2009 ASCE*, Oakland, California, USA, 1096–1107.

Bensi, M. T., Der Kiureghian, A., and Straub, D. (2011). *A Bayesian network methodology for infrastructure seismic risk assessment and decision support*. PEER 2011/02, Pacific Earthquake Engineering Research Center, University of California, Berkeley, USA.

Blume, S. W. (2007). *Electrical power system basics for the nonelectrical professional*. (E. H. Mohamed, ed.), IEEE press series on power engineering, John Wiley & Sons, Inc.,Hoboken, New Jersey.

Bobbio, A. (1999). “Comparing fault tree and baysian networks for dependability analysis.” *Computer Safety, Reliability, and Security: 18th International Conference, SAFECOMP 99*, Toulouse, France, 310–322.

Bobbio, A., Portinale, L., Minichino, M., and Ciancamerla, E. (2001). “Improving the analysis of dependable systems by mapping fault trees into Bayesian networks.” *Reliability Engineering and System Safety*, 71(3), 249–260.

Boore, D. M., Joyner, W. B., and Fumal, T. E. (1997). “Equations for estimating horizontal response spectra and peak acceleration from western North American earthquakes: a summary of recent work.” *Seismological Research Letters*, 68(1), 128–153.

Boudali, H., and Dugan, J. B. (2005). “A discrete-time Bayesian network reliability modeling and analysis framework.” *Reliability Engineering and System Safety*, 87(3), 337–349.

Buratti, N., Ferracuti, B., and Savoia, M. (2010). “Response surface with random factors for seismic fragility of reinforced concrete frames.” *Structural Safety*, 32(1), 42–51.

Campbell, K. W. (1997). “Empirical near-source attenuation relationships for horizontal and vertical components of peak ground acceleration , peak ground velocity , and pseudo-absolute acceleration response spectra.” *Seismological Research Letters*, 68(1), 154–179.

Cetin, K., Der Kiureghian, A., and Seed, R. B. (2002). “Probabilistic models for the Probabilistic models for the initiation of seismic soil liquefaction.” *Structural Safety*, 24(1), 67–82.

Chen, G., Yang, Z., and Sun, J. (2010). “Safety analysis of complex systems based on Bayesian netoworks.” *2nd International Conference on Industrial Mechatronics and Automation*, Wuhan, China, 92–95.

Cockburn, G., and Tesfamariam, S. (2012). “Earthquake disaster risk index for Canadian cities using Bayesian belief networks.” *Georisk: Assessment and Management of Risk for Engineered Systems and Geohazards*, 6(2), 128–140.

Dastous, J. B., Filiatrault, A., and Pierre, J. R. (2004). “Estimation of displacement at interconnection points of substation equipment subjected to earthquakes.” *IEEE Transactions on Power Delivery*, 19(2), 618–628.

De Souza, E., and Ochoa, P. M. (1992). “State space exploration in Markov models.” *Performance Evaluation Review*, 20(1), 152–166.

Der Kiureghian, A., Sackman, J. L., and Hong, K. J. (1999a). *Interaction in interconnected electrical substation equipment subjected to earthquake ground motions*. PEER 1999/01, Pacific Earthquake Engineering Research Center, University of California, Berkeley, USA.

Der Kiureghian, A., Sackman, J. L., and Hong, K. J. (1999b). *Further studies on seismic interaction on interconnected electrical substation equipment*. PEER 2000/01, Pacific Earthquake Engineering Research Center, University of California, Berkeley, USA.

Der Kiureghian, A., Sackman, J. L., and Hong, K. J. (2001). “Seismic interaction in linearly connected electrical substation equipment.” *Earthquake Engineering & Structural Dynamics*, 30(3), 327–347.

Design Expert V8. (2009). *Design-Expert® V8 software for Design of Experiments (DOE)*. Available from: http://www.statease.com/dx8descr.html [Last visited March 7, 2013].

Eidinger, J. M., and Ostrom, D. (1994). *Earthaquake loss estimation methods*. Technical manual, Electric power utilities, Prepared by G & E engineering systems Inc.

Eidinger, J., and Tang, A. K. (forthcoming). *Christchurch, New Zealand earthquake sequence of 2010 and 2011: lifeline performance*. Technical Council on Lifeline Earthquake Engineering Monograph, American Society of Civil Engineers, Reston, VA.

Enright, M. P., and Frangopol, D. M. (1999). “Maintenance planning for deterioration concrete bridges.” *Journal of Structural Engineering*, 125(12), 1407–1414.

Ersoy, S. (2001). “Analytical and experimental seismic studies of transformers isolated with friction pendulum system and design aspects.” *Earthquake Spectra*, 17(4), 569–595.

Ersoy, S. (2002). “Seismic response of transformer bushing systems and their rehabilitation using frictional pendulum system.” PhD Dissertation, New Jersey Institute of Technology, Newark, NJ, USA.

Ersoy, S., and Saadeghvaziri, M. A. (2004). “Seismic response of transformer-bushing systems.” *IEEE Transactions on Power Delivery*, 19(1), 131–137.

Feller, W. (1971). *Introduction to probability theory and its applications*. Wiley.

Filiatrault, A., and Matt, H. (2006). “Seismic response of high voltage electrical transformer-bushing systems.” *Journal of Structural Engineering*, 132(2), 287–295.

Gaunt, C. T., and Coetzee, G. (2007). “Transformer failures in regions incorrectly considered to have low GIC-risk.” *Power Tech, IEEE Lausanne*, Cape Town, South Africa, 807 – 812.

Gilani, A. S., Whittaker, A. S., Fenves, G. L., and Fujisaki, E. (1999a). *Seismic evaluation of 550 kV porcelain transformer bearings*. PEER 1999/05, Pacific Earthquake Engineering Research Center, University of California, Berkeley, USA.

Gilani, A. S., Whittaker, A. S., Fenves, G. L., and Fujisaki, E. (1999b). *Seismic evaluation and retrofit of 230-kV porcelain transformer bushings*. PEER 1999/14, Pacific Earthquake Engineering Research Center, University of California, Berkeley, USA.

Hong, K. J., Kiureghian, A. D., and Sackman, J. L. (2001). “Seismic interaction in cable-connected equipment items.” *Journal of Engineering Mechanics*, 127(11), 1096–1105.

Huo, J. R., and Hwang, H. H. M. (1995). *Seismic fragility analysis of equipment and structures in a Memphis electric substation*. Technical Report NCEER-95-0014, National Center for Earthquake Engineering Research, Buffalo, NY, USA.

Hwang, H. H. M., and Chou, T. (1998). “Evaluation of seismic performance of an electric substation using event tree/fault tree technique.” *Probabilistic Engineering Mechanics*, 13(2), 117–124.

IEEE-1527. (2006). *IEEE recommended practice for the design of flexible buswork located in seismically active areas*. Report IEEE 1527. Institute of Electrical and Electronic Engineering.

IEEE-693. (2005). *IEEE recommended practice for seismic design of substations*. Report IEEE 693. Institute of Electrical and Electronic Engineering.

Ismail, M. A., Sadiq, R., Soleymani, H. R., and Tesfamariam, S. (2011). "Developing a road performance index using a Bayesian belief network model." *Journal of the Franklin Institute*, 348(9), 2539–2555.

Jaigirdar, M. A. (2005). "Seismic fragility and risk analysis of electric power substations." Masters Thesis, Department of Civil and Applied Mechanics, McGill University, Montreal, Quebec.

Jensen, F. V. (1996). *An introduction to Bayesian networks*. UCL Press, London.

Khuri, A. I., and Mukhopadhyay, S. (2010). "Response surface methodology." *Wiley Interdisciplinary Reviews: Computational Statistics*, 2(2), 128–149.

Kuehn, N. M., Riggelsen, C., and Scherbaum, F. (2009). *Facilitating probabilistic seismic hazard analysis using Bayesian networks*. Seventh Annual Workshop on Bayes Applications (in conjunction with UAI/COLT/ICML 2009).

Langseth, H., and Portinale, L. (2007). "Bayesian networks in reliability." *Reliability Engineering and System Safety*, 92(1), 92–108.

Lee, B. H. (2001). "Using Bayes belief networks in industrial FMEA modeling and analysis." *International Symposium on Product Quality and Integrity*, CA, USA, 7–15.

Liu, K. F. R., Lu, C. F., Chen, C. W., and Shen, Y. S. (2011). "Applying Bayesian belief networks to health risk assessment." *Stochastic Environmental Research and Risk Assessment*, 26(3), 451–465.

Lounis, Z., Lacasse, M. A., Vanier, D. J., and Kyle, B. R. (1998). "Towards standardization of service life prediction of roofing membranes." *Roofing research and standards development: 4th. Volume, ASTM STP 1349*, T. J. Wallace and W. J. Rossiter, eds., American Society for Testing and Materials.

Mahadevan, S., Zhang, R., and Smith, N. (2001). "Bayesian networks for system reliability reassessment." *Structural Safety*, 23(3), 231–251.

Makris, N., and Black, C. J. (2001). *Rocking response of equipment anchored to a base foundation*. PEER 2001/14, Pacific Earthquake Engineering Research Center, University of California, Berkeley, USA.

Makris, N., and Black, C. J. (2002). "Uplifting and overturning of equipment anchored to a base foundation." *Earthquake Spectra*, 18(4), 631–661.

Makris, N., and Roussos, Y. (1998). *Rocking response and overturning of equipment under horizontal pulse-type motions*. PEER 1998/05, Pacific Earthquake Engineering Research Center, University of California, Berkeley, USA.

Makris, N., and Roussos, Y. (2000). "Rocking response of rigid blocks under near-source ground motions." *Géotechnique*, 50(3), 243–262.

Makris, N., and Zhang, J. (1999). *Rocking response and overturning of anchored equipment under seismic excitations*. PEER 1999/06, Pacific Earthquake Engineering Research Center, University of California, Berkeley, USA.

Makris, N., and Zhang, J. (2001). "Rocking response of anchored blocks under pulse-type motions." *Journal of Engineering Mechanics*, 127(5), 484–493.

Matsuda, E. N., Savage, W. U., Williams, K. K., and Laguens, G. C. (1991). "Earthquake evaluation of a substation network." *Third U.S Conference on Lifeline Earthquake Engineering, ASCE*, New York, USA, 295–317.

McCann, R. K., Marcot, B. G., and Ellis, R. (2006). "Bayesian belief networks: applications in ecology and natural resource." *Canadian Journal of Forest Research*, 36(12), 3053–3062.

Mitchell, D., Tinawi, R., and Law, T. (1990). "Damage caused by the November 25, 1988, Saguenay earthquake." *Canadian Journal of Civil Engineering*, 17(3), 338–365.

Möller, O., Foschi, R. O., Rubinstein, M., and Quiroz, L. (2009). "Seismic structural reliability using different nonlinear dynamic response surface approximations." *Structural Safety*, 31(5), 432–442.

Morales, E. M., and Morales, M. K. (2003). *State of practice in soil liquefaction mitigation and engineering countermeasures*. Available in: http://www.pgatech.com.ph/State of Practice in Soil Liquefaction Mitigation.pdf, 1–29.

Morcous, G. (2006). "Performance prediction of bridge deck systems using Markov chains." *Journal of Performance of Constructed Facilities*, 20(2), 146–155.

Morcous, G., and Lounis, Z. (2007). "Probabilistic and mechanistic deterioration models for bridge management." *Computing in Civil Engineering*, Pittsburgh, Pennsylvania, United States, 364–373.

Norsys Software Corp. (2006). *Netica TM application [online]*. Available from: http://www.norsys.com [Last visited February 12, 2013].

Nuti, C., Rasulo, A., and Vanzi, I. (2007). "Seismic safety evaluation of electric power supply at urban level." *Earthquake Engineering & Structural Dynamics*, 36(2), 245–263.

Paolacci, F., and Giannini, R. (2009). “Seismic reliability assessment of a high-voltage disconnect switch using an effective fragility analysis.” *Journal of Earthquake Engineering*, 13(2), 217–235.

Parzen, E. (1962). *Stochastic processes*. Holden Day, San Francisco.

Pearl, J. (1988). *Probabilistic reasoning in intelligent systems: network of plausible inference*. Morgan Kaufmann Publishers, Inc., San Francisco, CA.

PEER. (2005). *Pacific earthquake engineering research center: NGA database*. Available in: http://peer.berkeley.edu/nga/ [Last visited: February 11, 2013].

Porter, K. A., Krishnan, S., and Xu, X. (2006). *Analysis of simultaneous operational failure of critical facilities due to earthquake, for a California utility*. Report no. EERL 2006-01, California Institute of Technology, Earthquake Engineering Research Laboratory.

Rajeev, P., and Tesfamariam, S. (2012). “Seismic fragilities for reinforced concrete buildings with consideration of irregularities.” *Structural Safety*, 39, 1–13.

Saadeghvaziri, M. A., Feizi, B., Jr, L. K., and Alston, D. (2010). “On seismic response of substation equipment and application of base isolation to transformers.” *IEEE Transactions on Power Delivery*, 25(1), 177–186.

Sadigh, K., Chang, C. Y., Egan, J. A., Makdisi, F., and Youngs, R. R. (1997). “Attenuation relationships for shallow crustal earthquakes based on California strong motion data.” *Seismological Research Letters*, 68(1), 180–189.

Schiff, A. J. (1997). *Northridge earthquake: lifeline performance and post-earthquake response*. (Anshel J Schiff, ed.), Technical Council on Lifeline Earthquake Engineering, Monograph No. 8, ASCE, New York, USA.

Schiff, A J. (1998). *The Loma Prieta, California, earthquake of October 17, 1989-lifelines*. U.S Geological Survey Professional Paper 1552-A.

Schiff, A J. (2003). “Chapter 25: Electrical power systems.” *Earthquake engineering handbook*, C. Wai-Fah and S. Charles, eds., CRC Press, USA.

Seed, H. B., and Idriss, I. M. (1971). “Simplified procedure for evaluating soil liquefaction potential.” *Journal of Soil Mechanics and Foundations Division*, 97(9), 1249–1273.

Shenton, W. (1996). “Criteria for initiation of slide, rock, and slide-rock rigid-body modes.” *Journal ofEngineering Mechanics*, 122(7), 690–693.

Shi, X. M., and Wang, H. W. (2004). “FMEA model of complex system based on Bayesian networks.” *Ordnance Industry Automation*, Vol. II.

Song, J., Der Kiureghian, A., and Sackman, J. L. (2004). *Seismic response and reliability of electrical substation equipment and systems*. PEER 2005/16, Pacific Earthquake Engineering Research Center, University of California, Berkeley, USA.

Song, J., Der Kiureghian, A., and Sackman, J. L. (2007). "Seismic interaction in electrical substation equipment connected by non-linear rigid bus conductors." *Earthquake Engineering and Structural Dynamics*, 36(2), 167–190.

Stewart, R. P., Fronk, R., and Jurbin, T. (2003). "Chapter 13: Seismic considerations." *Electric power substation engineering*, J. D. McDonald, ed., CRC PRESS, Washington, D.C.

Straub, D., and Der Kiureghian, A. (2008). "Improved seismic fragility modeling from empirical data." *Structural Safety*, 30(4), 320–336.

Straub, D., and Der Kiureghian, A. (2010a). "Bayesian network enhanced with structural reliability methods: methodology." *Journal of Engineering Mechanics*, 136(10), 1248–1258.

Straub, D., and Der Kiureghian, A. (2010b). "Bayesian network enhanced with structural reliability methods: application." *Journal of Engineering Mechanics*, 136(10), 1259–1270.

Sušnik, J., Vamvakeridou-Lyroudia, L., Kapelan, Z., and Savić, D. A. (2010). "Major risk categories and associated critical risk event trees to quantify." Report number: 2011.003, Report prepared for the project "PREPARED Enabling Change."

Tesfamariam, S., Hurlburt, G., Sun, J., and Siraj, T. (2011). "Seismic induced building damage assessment using bayesian belief network." *CSCE 2011 General Conference*, Ottawa, Ontario, Canada.

Tesfamariam, S., and Liu, Z. (2013). "Seismic risk analysis using Bayesian belief networks." *Handbook of seismic risk analysis and management of civil infrastructure systems*, S. Tesfamariam and K. Goda, eds., Woodhead Publishing Limited, Cambridge, UK.

Tesfamariam, S., and Martín-Pérez, B. (2009). "Bayesian belief network to assess Carbonation-induced corrosion in reinforced concrete." *Journal of Materials in Civil Engineering*, 20(11), 707–717.

Timothy, D., and Scott, M. O. (1995). "Liquefaction resistance using CPT and field case histories." *Journal of Geotechnial engineering*, 121(12), 856–869.

Toro, G. R., Abrahamson, N. A., and Schneider, J. F. (1997). "Model of strong ground motions from earthquakes in central and eastern North America: best estimates and uncertainties." *Seismological Research Letters*, 68(1), 41–57.

United States Department of Energy. (2004). *Final report on the August 14, 2003 blackout in the United states and Canada: causes and recommendations*. U.S.Canada power system outage task force.

Uusitalo, L. (2007). "Advantages and challenges of Bayesian networks in environmental modelling." *Ecological Modelling*, 203(3-4), 312–318.

Wakefield, R. R., and Sears, G. A. (1997). "Petri nets for simulation and modeling of construction systems." *Journal of Construction Engineering and Management*, 123(2), 105–112.

Weber, P., Medina-Oliva, G., Simon, C., and Iung, B. (2010). "Overview on Bayesian networks applications for dependability, risk analysis and maintenance areas." *Engineering Applications of Artificial Intelligence*, 25(4), 671–682.

Whittaker, A. S., Fenves, G. L., and Gilani, A. S. (2004). "Earthquake performance of porcelain transformer bushings." *Earthquake Spectra*, 20(1), 205–223.

Whittaker, A. S., Fenves, G. L., and Gilani, A. S. (2007). "Seismic evaluation and analysis of high-voltage substation disconnect switches." *Engineering Stuctures*, 29(12), 3538–3549.

Yang, S., Lu, M., Liu, B., and Hao, B. (2009). "A fault diagnosis model for embedded software based on FMEA/FTA and bayesian network." *8th International Conference on Reliability, Maintainability and Safety*, Beijing, China, 778–782.

Yi, H., Jiang, C., Hu, H., Cai, K., and Mathur, A. P. (2011). "Using Markov-chains to model reliability and QoS for deployed service-based systems." *2011 IEEE 35th Annual Computer Software and Applications Conference Workshops*, Ieee, Beijing, China, 356–361.

Youd, T. L., Idriss, I. M., Andrus, R. D., Arango, I., Castro, G., Christian, J. T., Dobry, R., Finn, W. D., Harder, L. F. J., Hynes, M. E., Ishihara, K., Koester, J. P., Liao, S. S. C., Marcuson III, W. F., Martin, G. R., Mitchell, J. K., Moriwaki, Y., Power, M. S., Robertson, P. K., Seed, R. B., and Stokoe II, K. H. (2001). "Liquefaction resistance of soils: summary report from the 1996 NCEER and 1998 NCEER/NSF workshops on evaluation of liquefaction resistance of soils." *Journal of Geotechnical and Geoenvironmental Engineering*, 127(10), 817–833.

Youngs, R. R., Chiou, S. J., Silva, W. J., and Humphrey, J. R. (1997). "Strong ground motion attenuation relationships for subduction zone earthquakes." *Seismological Research Letters*, 68(1), 59–73.

Zhou, L., Yan, G., and Ou, J. (2013). "Response surface method based on radial basis functions for modeling large-scale structures in model updating." *Computer-Aided Civil and Infrastructure Engineering*, 28(3), 210–226.

Appendices

Appendix A: NEHRP Site Class with Recommended Values of Average Shear-wave Velocity

Site	Soil Profile Name	V_{s30} Recommended (m/sec)	NEHRP V_{s30} Range (m/sec)
NEHRP class A	Hard rock	1890	> 1500
NEHRP class B	Rock	1070	760 to 1500
NEHRP class C	Very dense soil and soft rock	520	360 to 760
NEHRP class D	Stiff soil profile	250	180 to 360
NEHRP class E	Soft soil profile	150	< 180

*Note: The provided information is available in: *http://peer.berkeley.edu/course_modules/eqrd/index.htm?c227top.htm&227cont.htm&IntExmp/atten00.htm* (Last visited February 11, 2013)

Appendix B: Description of the CPT for Node Variable "Conductor Failure"

(ECL, RCL)	Conductor failure (UL_{CF}, L_{CF}, VL_{CF})
($VL_{1\text{-}150}$, $VL_{1\text{-}150}$)	(80, 20, 0)
($VL_{1\text{-}150}$, $L_{150\text{-}300}$)	(40, 50, 10)
($VL_{1\text{-}150}$, $M_{300\text{-}450}$)	(5, 20, 75)
($VL_{1\text{-}150}$, $H_{450\text{-}700}$)	(0, 15, 85)
($VL_{1\text{-}150}$, $VH_{700\text{-}1000}$)	(0, 5, 95)
($L_{150\text{-}300}$, $VL_{1\text{-}150}$)	(90, 10, 0)
($L_{150\text{-}300}$, $L_{150\text{-}300}$)	(80, 10, 10)
($L_{150\text{-}300}$, $M_{300\text{-}450}$)	(5, 30, 65)
($L_{150\text{-}300}$, $H_{450\text{-}700}$)	(5, 20, 75)
($L_{150\text{-}300}$, $VH_{700\text{-}1000}$)	(0, 15, 85)
($M_{300\text{-}450}$, $VL_{1\text{-}150}$)	(90, 10, 0)
($M_{300\text{-}450}$, $L_{150\text{-}300}$)	(80, 15, 5)
($M_{300\text{-}450}$, $M_{300\text{-}450}$)	(70, 20, 10)
($M_{300\text{-}450}$, $H_{450\text{-}700}$)	(25, 30, 45)
($M_{300\text{-}450}$, $VH_{700\text{-}1000}$)	(10, 15, 75)
($H_{450\text{-}700}$, $VL_{1\text{-}150}$)	(95, 5, 0)
($H_{450\text{-}700}$, $L_{150\text{-}300}$)	(85, 10, 5)
($H_{450\text{-}700}$, $M_{300\text{-}450}$)	(80, 15, 5)
($H_{450\text{-}700}$, $H_{450\text{-}700}$)	(65, 25, 10)
($H_{450\text{-}700}$, $VH_{700\text{-}1000}$)	(25, 30, 45)
($VH_{700\text{-}1000}$, $VL_{1\text{-}150}$)	(98, 2, 0)
($VH_{700\text{-}1000}$, $L_{150\text{-}300}$)	(95, 5, 0)
($VH_{700\text{-}1000}$, $M_{300\text{-}450}$)	(85, 10, 5)
($VH_{700\text{-}1000}$, $H_{450\text{-}700}$)	(75, 20, 5)
($VH_{700\text{-}1000}$, $VH_{700\text{-}1000}$)	(60, 30, 10)

Appendix C: Description of the CPT for Node Variable "Rocking Response of Transformer"

(PGA, B/H, μ_s)	RT (Rest, Slide, Rock)
(Extremely Low, $A_{0.34}$, Anchored, 0.45)	(100, 0, 0)
(Extremely Low, $B_{0.39}$, Anchored, 0.45)	(100, 0, 0)
(Extremely Low, $C_{0.42}$, Anchored, 0.45)	(100, 0, 0)
(Extremely Low, $D_{0.43}$, Anchored, 0.45)	(100, 0, 0)
(Extremely Low, $E_{0.50}$, Anchored, 0.45)	(100, 0, 0)
(Extremely Low, $F_{0.51}$, Anchored, 0.45)	(100, 0, 0)
(Extremely Low, $G_{0.65}$, Anchored, 0.45)	(100, 0, 0)
(Extremely Low, $H_{0.69}$, Anchored, 0.45)	(100, 0, 0)
(Very Low, $A_{0.34}$, Anchored, 0.45)	(100, 0, 0)
(Very Low, $B_{0.39}$, Anchored, 0.45)	(100, 0, 0)
(Very Low, $C_{0.42}$, Anchored, 0.45)	(100, 0, 0)
(Very Low, $D_{0.43}$, Anchored, 0.45)	(100, 0, 0)
(Very Low, $E_{0.50}$, Anchored, 0.45)	(100, 0, 0)
(Very Low, $F_{0.51}$, Anchored, 0.45)	(100, 0, 0)
(Very Low, $G_{0.65}$, Anchored, 0.45)	(100, 0, 0)
(Very Low, $H_{0.69}$, Anchored, 0.45)	(100, 0, 0)
(Low, $A_{0.34}$, Anchored, 0.45)	(100, 0, 0)
(Low, $B_{0.39}$, Anchored, 0.45)	(100, 0, 0)
(Low, $C_{0.42}$, Anchored, 0.45)	(100, 0, 0)
(Low, $D_{0.43}$, Anchored, 0.45)	(100, 0, 0)
(Low, $E_{0.50}$, Anchored, 0.45)	(100, 0, 0)
(Low, $F_{0.51}$, Anchored, 0.45)	(100, 0, 0)
(Low, $G_{0.65}$, Anchored, 0.45)	(100, 0, 0)
(Low, $H_{0.69}$, Anchored, 0.45)	(100, 0, 0)
(Medium, $A_{0.34}$, Anchored, 0.45)	(100, 0, 0)
(Medium, $B_{0.39}$, Anchored, 0.45)	(99, 1, 0)
(Medium, $C_{0.42}$, Anchored, 0.45)	(99, 1, 0)
(Medium, $D_{0.43}$, Anchored, 0.45)	(99, 1, 0)
(Medium, $E_{0.50}$, Anchored, 0.45)	(99, 1, 0)
(Medium, $F_{0.51}$, Anchored, 0.45)	(99, 1, 0)
(Medium, $G_{0.65}$, Anchored, 0.45)	(100, 0, 0)
(Medium, $H_{0.69}$, Anchored, 0.45)	(100, 0, 0)
(High, $A_{0.34}$, Anchored, 0.45)	(99, 1, 0)
(High, $B_{0.39}$, Anchored, 0.45)	(85, 7.5, 7.5)
(High, $C_{0.42}$, Anchored, 0.45)	(85, 15, 0)
(High, $D_{0.43}$, Anchored, 0.45)	(0, 44, 56)
(High, $E_{0.50}$, Anchored, 0.45)	(95, 0, 5)

(PGA, B/H, μ_s)	**RT (Rest, Slide, Rock)**
(High, $F_{0.51}$, Anchored, 0.45)	(95, 0, 5)
(High, $G_{0.65}$, Anchored, 0.45)	(99, 1, 0)
(High, $H_{0.69}$, Anchored, 0.45)	(99, 1, 0)
(Very High, $A_{0.34}$, Anchored, 0.45)	(48, 10, 42)
(Very High, $B_{0.39}$, Anchored, 0.45)	(50, 15, 35)
(Very High, $C_{0.42}$, Anchored, 0.45)	(54, 16, 30)
(Very High, $D_{0.43}$, Anchored, 0.45)	(55, 16, 29)
(Very High, $E_{0.50}$, Anchored, 0.45)	(60, 25, 15)
(Very High, $F_{0.51}$, Anchored, 0.45)	(61, 28, 11)
(Very High, $G_{0.65}$, Anchored, 0.45)	(69, 30, 1)
(Very High, $H_{0.69}$, Anchored, 0.45)	(69, 31, 0)
(Extremely High, $A_{0.34}$, Anchored, 0.45)	(43, 12, 45)
(Extremely High, $B_{0.39}$, Anchored, 0.45)	(38, 22, 40)
(Extremely High, $C_{0.42}$, Anchored, 0.45)	(40, 43, 57)
(Extremely High, $D_{0.43}$, Anchored, 0.45)	(42, 26, 32)
(Extremely High, $E_{0.50}$, Anchored, 0.45)	(40, 32, 28)
(Extremely High, $F_{0.51}$, Anchored, 0.45)	(48, 34, 18)
(Extremely High, $G_{0.65}$, Anchored, 0.45)	(50, 45, 5)
(Extremely High, $H_{0.69}$, Anchored, 0.45)	(50, 49, 1)
(Extremely Extremely High, $A_{0.34}$, Anchored, 0.45)	(25, 15, 60)
(Extremely Extremely High, $B_{0.39}$, Anchored, 0.45)	(25, 25, 50)
(Extremely Extremely High, $C_{0.42}$, Anchored, 0.45)	(30, 30, 40)
(Extremely Extremely High, $D_{0.43}$, Anchored, 0.45)	(30, 32, 38)
(Extremely Extremely High, $E_{0.50}$, Anchored, 0.45)	(35, 35, 30)
(Extremely Extremely High, $F_{0.51}$, Anchored, 0.45)	(38, 42, 20)
(Extremely Extremely High, $G_{0.65}$, Anchored, 0.45)	(38, 54, 8)
(Extremely Extremely High, $H_{0.69}$, Anchored, 0.45)	(39, 59, 2)